CPAN
Ingenio 2010

IGFAE
INSTITUTO GALEGO
DE FÍSICA
DE ALTAS ENERXÍAS

25 1999 2024

Photoactivation of ^{209}Bi with laser-induced bremsstrahlung

Adrián Bembibre Fernández

adrian.bembibre.fernandez@usc.es

Acknowledgements

A. Alejo

J. Benlliure

A. Junghans

A. Irman, Y.-Y. Chang, F. Herrmann, M. Laberge, J. Metzkes, S. Schöbel, K. Zeil, P. Ufer, T. Cowan, U. Schramm

Work supported by the Xunta de Galicia grant ED431F2023/21, by "la Caixa" Foundation (ID 100010434) (fellowship code LCF/BQ/PI20/11760027), FPI grant PRE2019-090730 within the project RTI2018-101578-B-C21 and grant RYC2021-032654I funded by MICIU/AEI/10.13039/501100011033 and by "European Union NextGenerationEU".

This project has received funding from the Euroatom research and training programme 2014-2018 under grant agreement No. 847594 (ARIEL)

María de Maeztu grant CEX2023- 001318-M funded by MICIU/AEI /10.13039/501100011033.

This work has received financial support from the Xunta de Galicia (CIGUS Network of Research Centres) and the European Union

Outline

- Introduction
- Experimental photon source
- Demonstration of a photoreaction experiment
- Conclusions

Introduction

Motivation

- Data of photon-induced reactions is of high interest for their applications, such as:
  - Radiation protection in planetary exploration.
  - New schemes of medical radioisotope production (theranostics…).
  - γ imaging.
  - …

Motivation

- Data of photon-induced reactions is of high interest for their applications, such as:
  - Radiation protection in planetary exploration.
  - New schemes of medical radioisotope production (theranostics…).
  - γ imaging.
  - …
- Experiments are needed to further extend the data available.
- Typically, these experiments take place in conventional accelerators.

Motivation

- Data of photon-induced reactions is of high interest for their applications, such as:
  - Radiation protection in planetary exploration.
  - New schemes of medical radioisotope production (theranostics…).
  - γ imaging.
  - …
- Experiments are needed to further extend the data available.
- Typically, these experiments take place in conventional accelerators.

Is there any limitation?

Motivation

- Drawbacks of conventional accelerators, such as LINACS, for high-energy photons production:
  - Limited access because of the high demand.
  - In most facilities, maximum energies up to 100 MeV.
  - Large and expensive.

Motivation

- Drawbacks of conventional accelerators, such as LINACS, for high-energy photons production:
  - Limited access because of the high demand.
  - In most facilities, maximum energies up to 100 MeV.
  - Large and expensive.
- Laser-based sources are an alternative for small-scale experiments:
  - Increase the number of facilities available.
  - Reduced footprint.
  - More affordable in terms of building and operation.
  - Photons of up to hundreds of MeV.

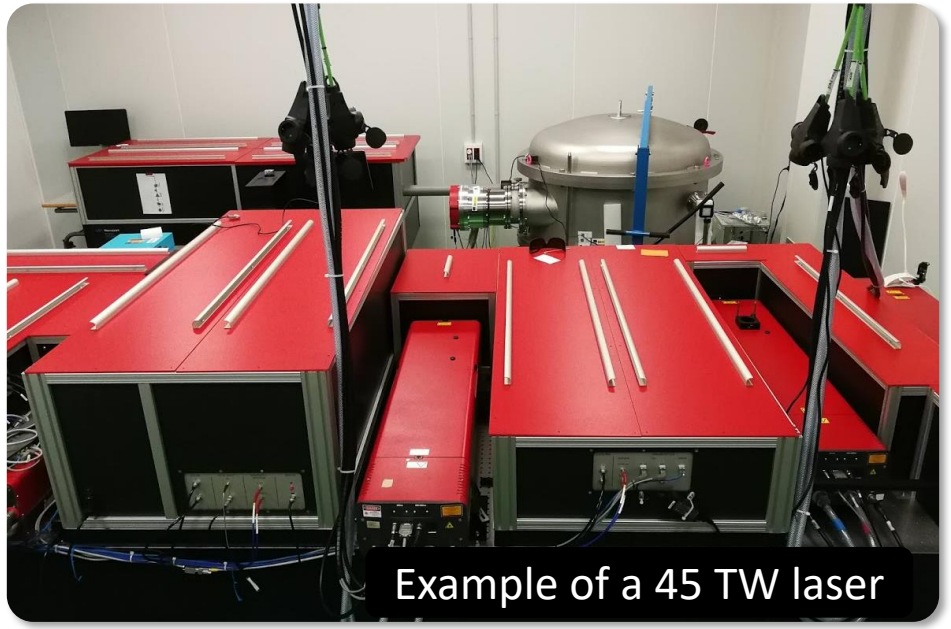
Example of a 45 TW laser

Motivation

- Drawbacks of conventional accelerators, such as LINACS, for high-energy photons production:
  - Limited access because of the high demand.
  - In most facilities, maximum energies up to 100 MeV.
  - Large and expensive.
- Laser-based sources are an alternative for small-scale experiments:
  - Increase the number of facilities available.
  - Reduced footprint.
  - More affordable in terms of building and operation.
  - Photons of up to hundreds of MeV.

How can we use them?

Laser-driven electron beams

- Laser wakefield (LWFA) is the most studied electron acceleration mechanism:
  - The laser impinges in a plasma pushing electrons aside generating a wave pattern.
  - When electrons are trapped in those waves, they can “surf” them and gain energy.
  - Compact accelerators: acceleration gradients up to GV/cm (vs <0.001 GV/cm in conventional accelerators).
  - Current energy record (reported): 8 GeV from 20 cm stage (Gonsalves *et al*., PRL 2019).

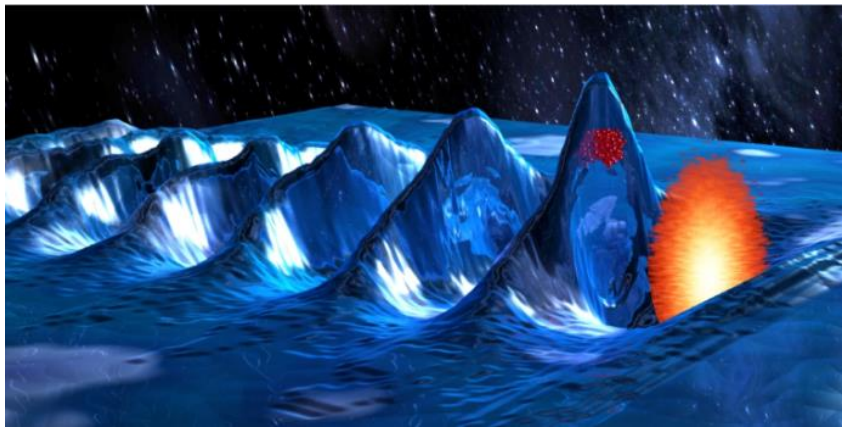

Laser-driven electron beams

- Laser wakefield (LWFA) is the most studied electron acceleration mechanism:
  - The laser impinges in a plasma pushing electrons aside generating a wave pattern.
  - When electrons are trapped in those waves, they can “surf” them and gain energy.
  - Compact accelerators: acceleration gradients up to GV/cm (vs <0.001 GV/cm in conventional accelerators).
  - Current energy record (reported): 8 GeV from 20 cm stage (Gonsalves *et al*., PRL 2019).

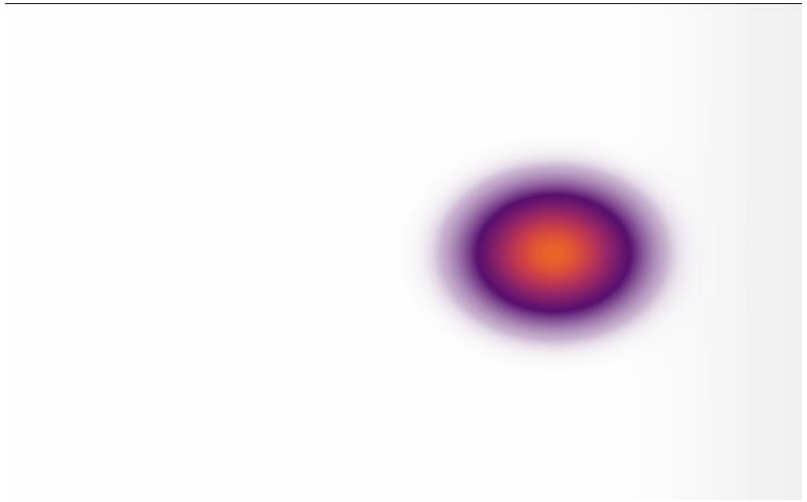

Laser-driven electron beams

- Laser wakefield (LWFA) is the most studied electron acceleration mechanism:
  - The laser impinges in a plasma pushing electrons aside generating a wave pattern.
  - When electrons are trapped in those waves, they can “surf” them and gain energy.
  - Compact accelerators: acceleration gradients up to GV/cm (vs <0.001 GV/cm in conventional accelerators).
  - Current energy record (reported): 8 GeV from 20 cm stage (Gonsalves *et al*., PRL 2019).
- Those electrons can be transformed into high-energy photons using a high-Z converter.

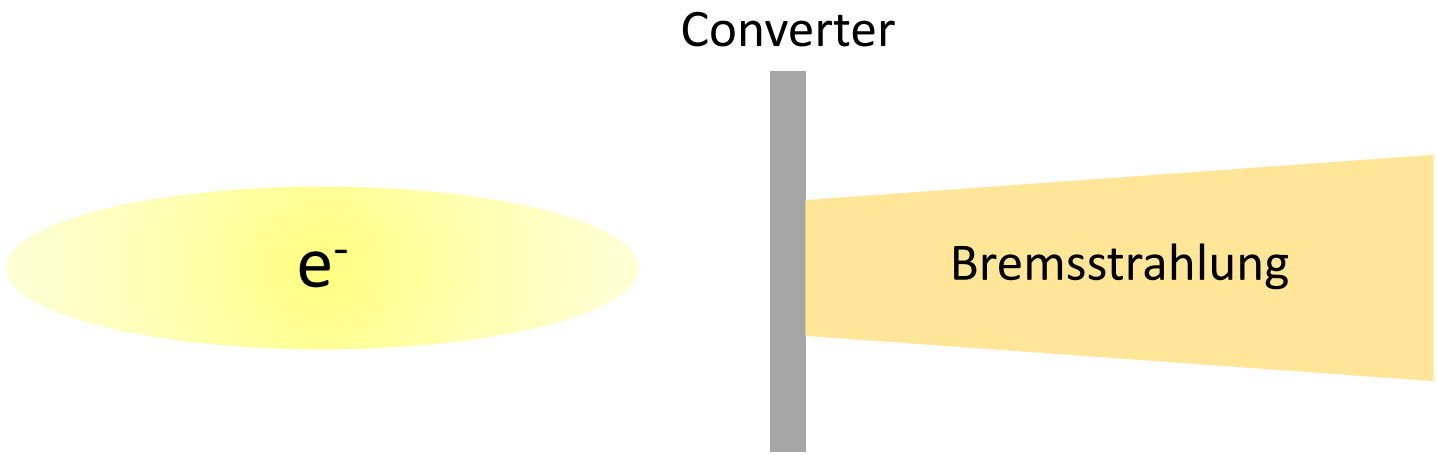

Experimental photon source

Electron source

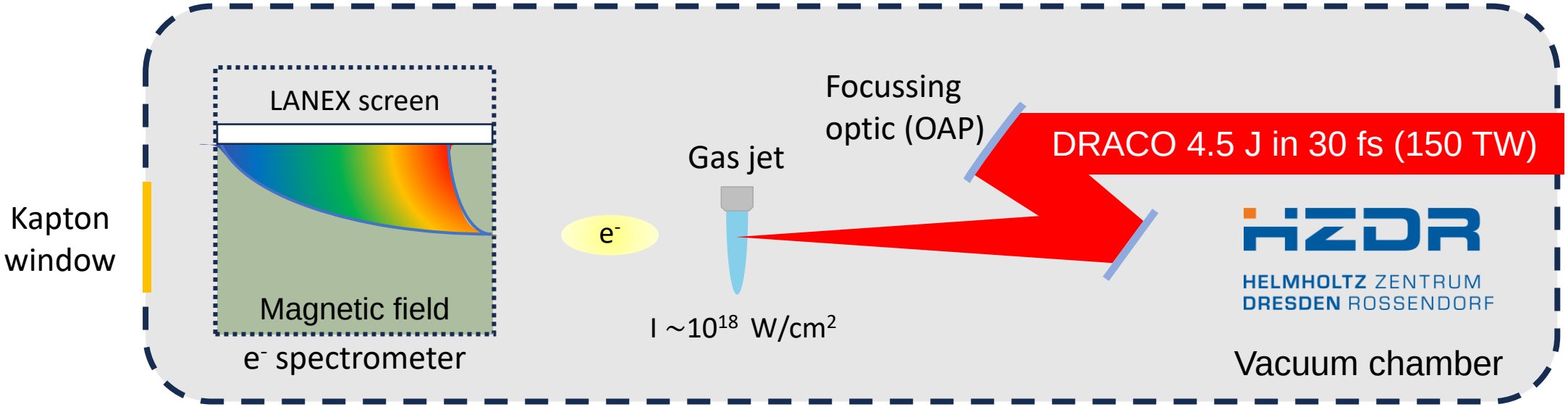

- Electron spectrometer before and after irradiation for beam characterisation

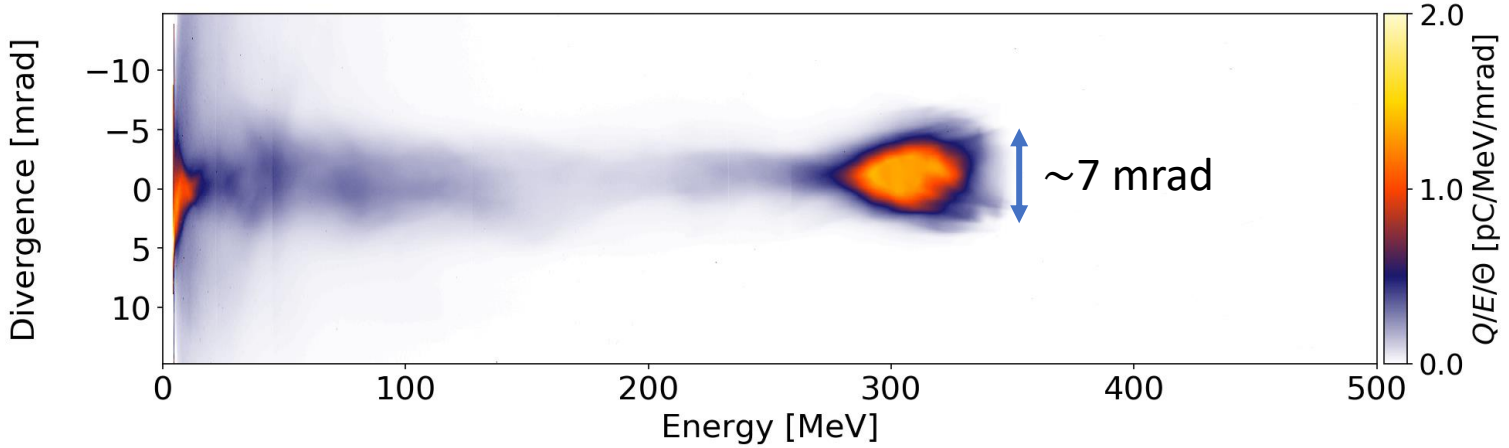

Electron source

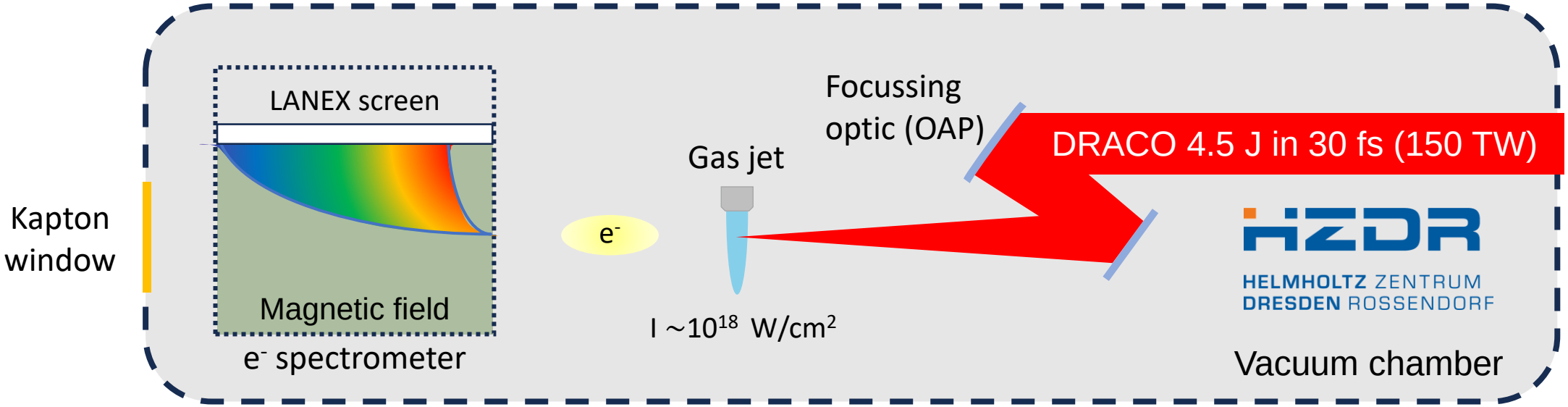

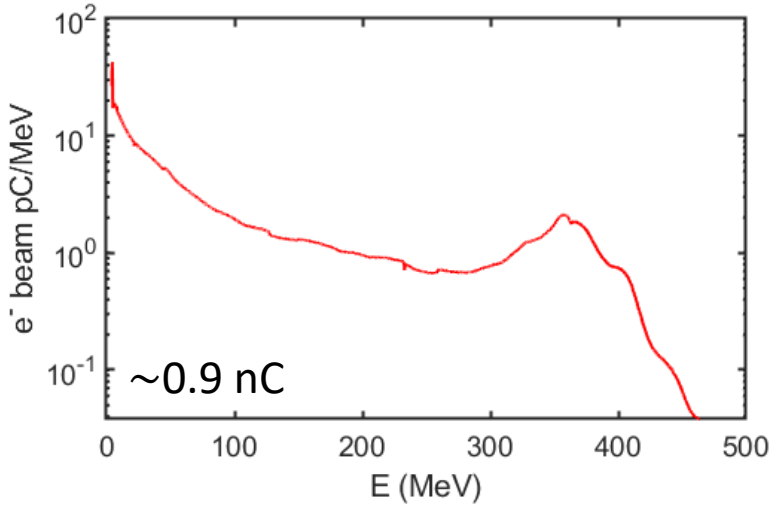

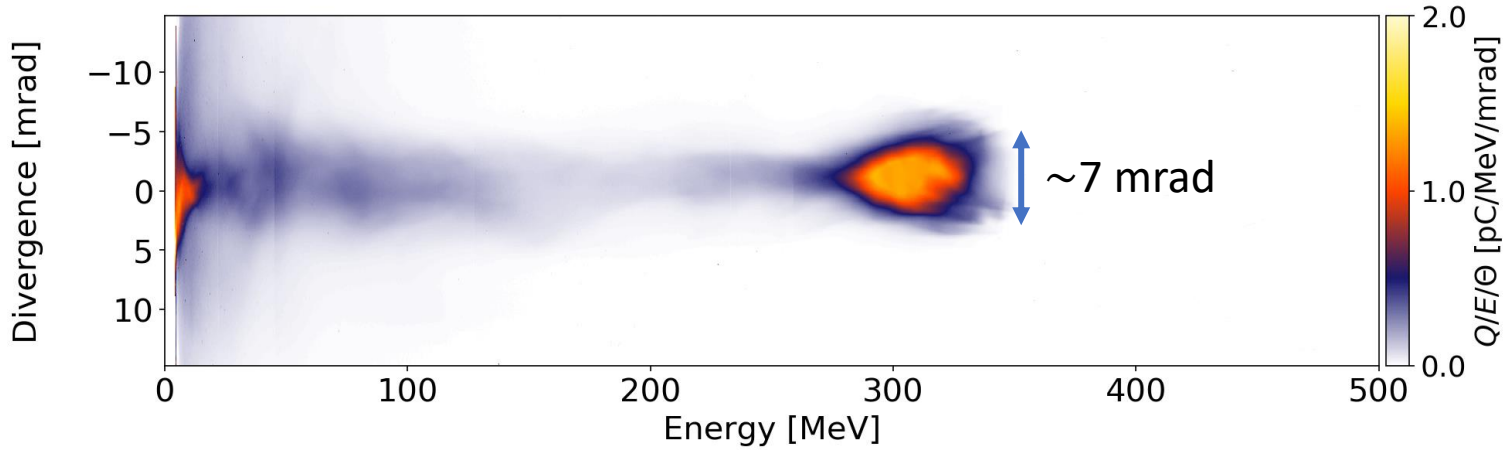

Bremsstrahlung source

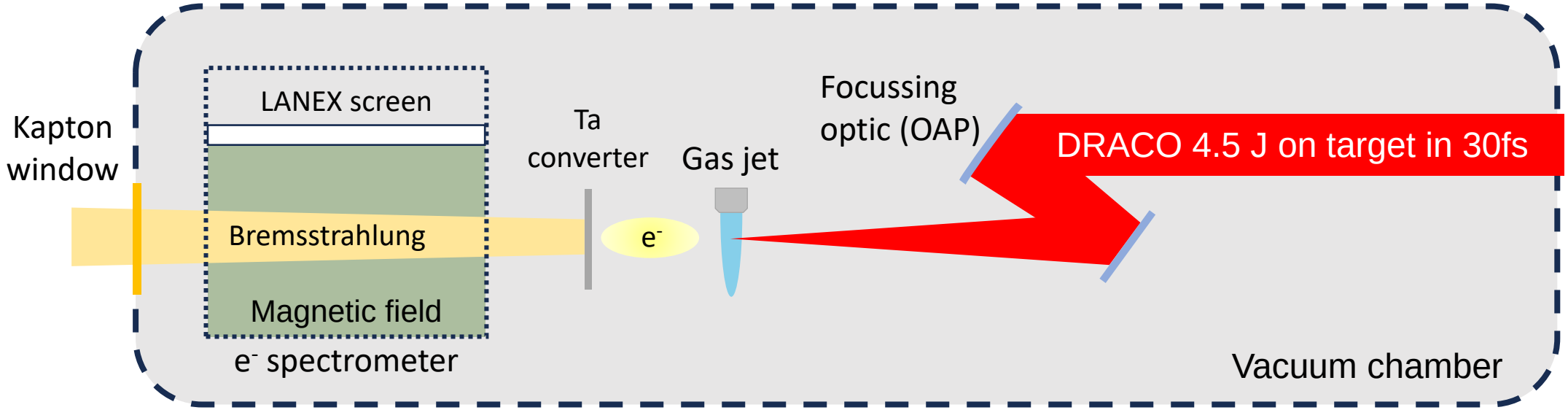

- For bremsstrahlung production a 0.8 mm tantalum converter was placed.
- Electrons were deflected with a magnet.
- Bremsstrahlung spectrum **could not be measured** → Numerical simulation

Bremsstrahlung source

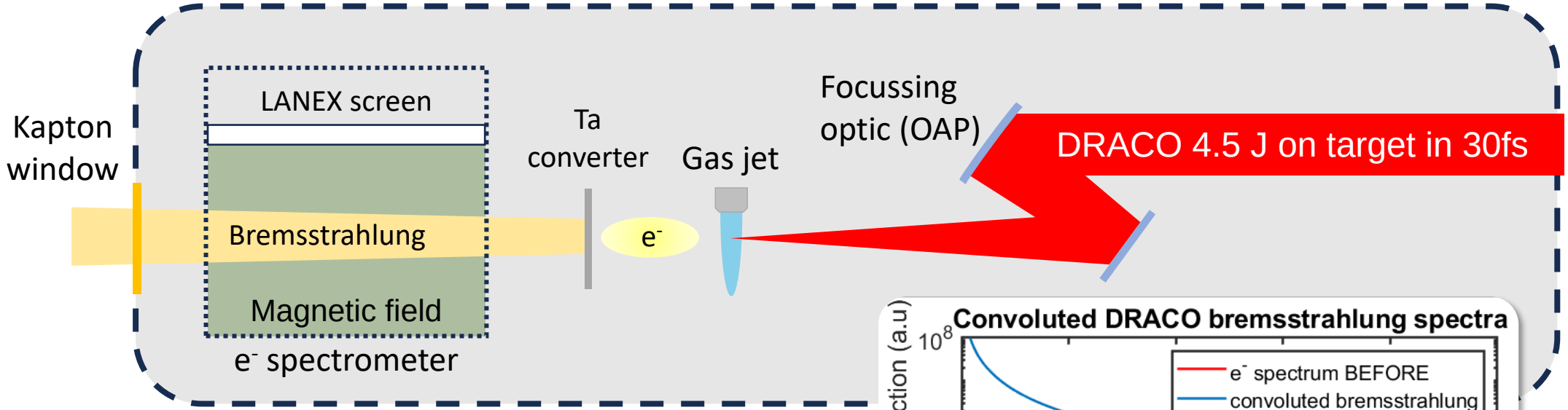

- For bremsstrahlung production a 0.8 mm tantalum converter was placed.
- Electrons were deflected with a magnet.
- Bremsstrahlung spectrum **could not be measured** → Numerical simulation

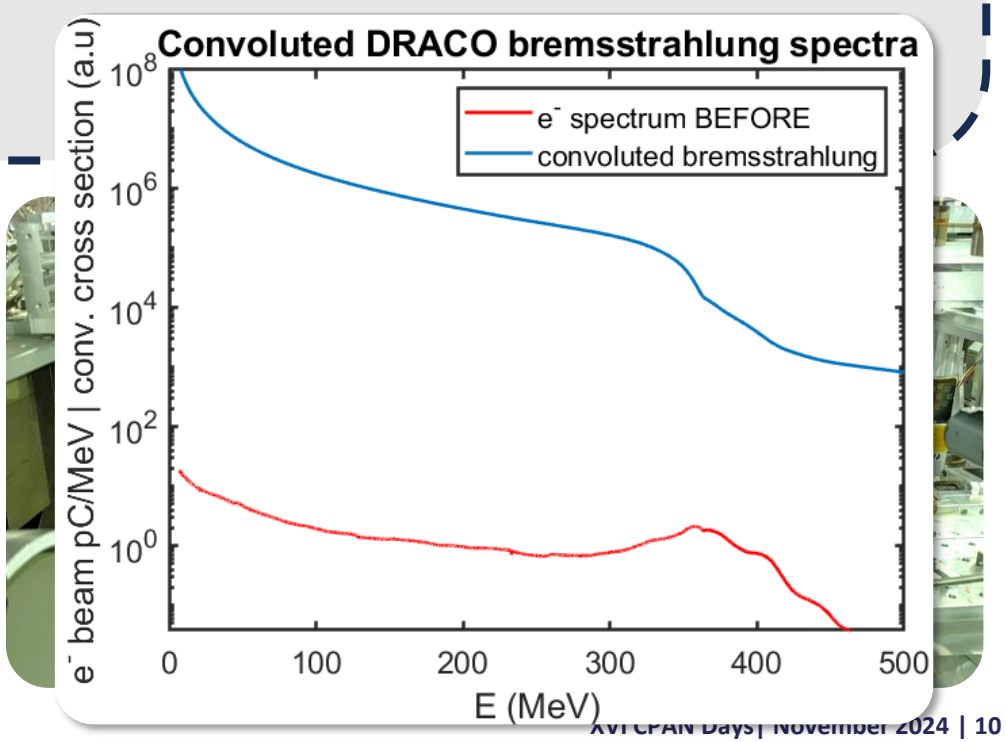

Sample irradiation

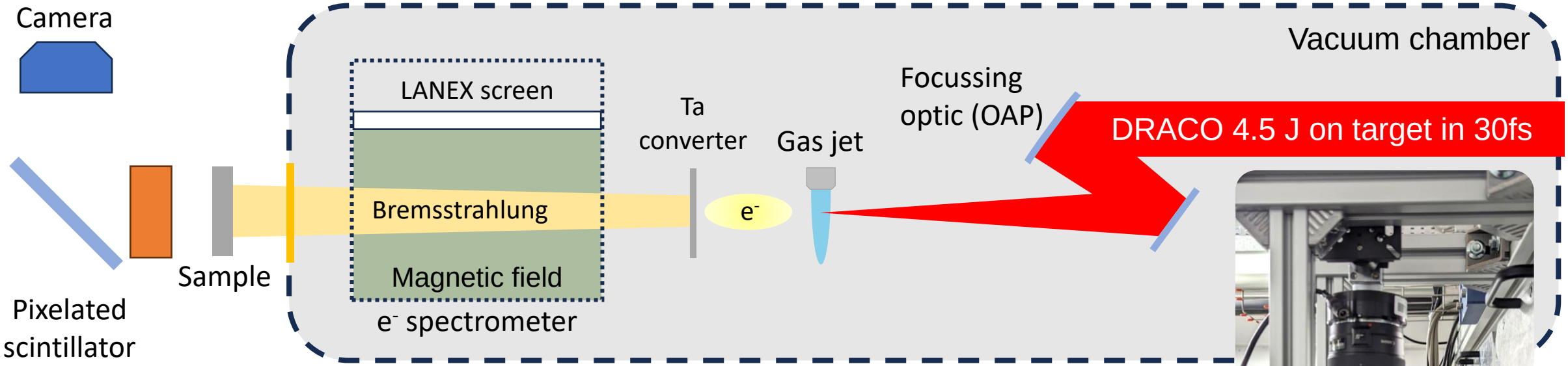

- Sample placed outside the chamber after a 125 µm Kapton window.
- Bremsstrahlung pointing measured online with a pixelated scintillator placed after the sample.

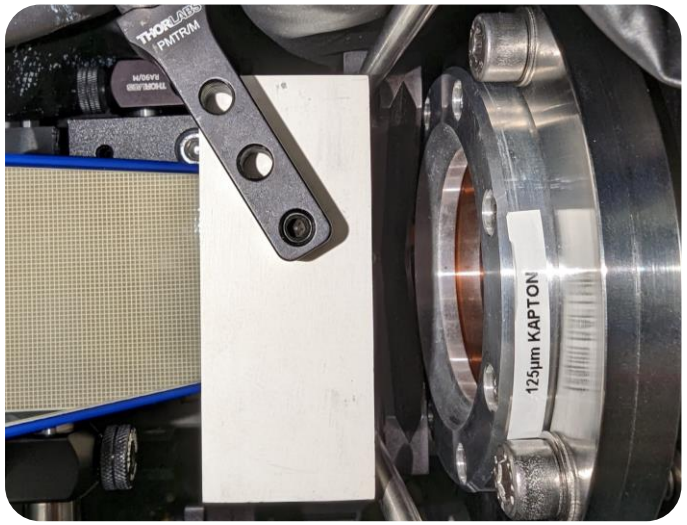

Sample irradiation

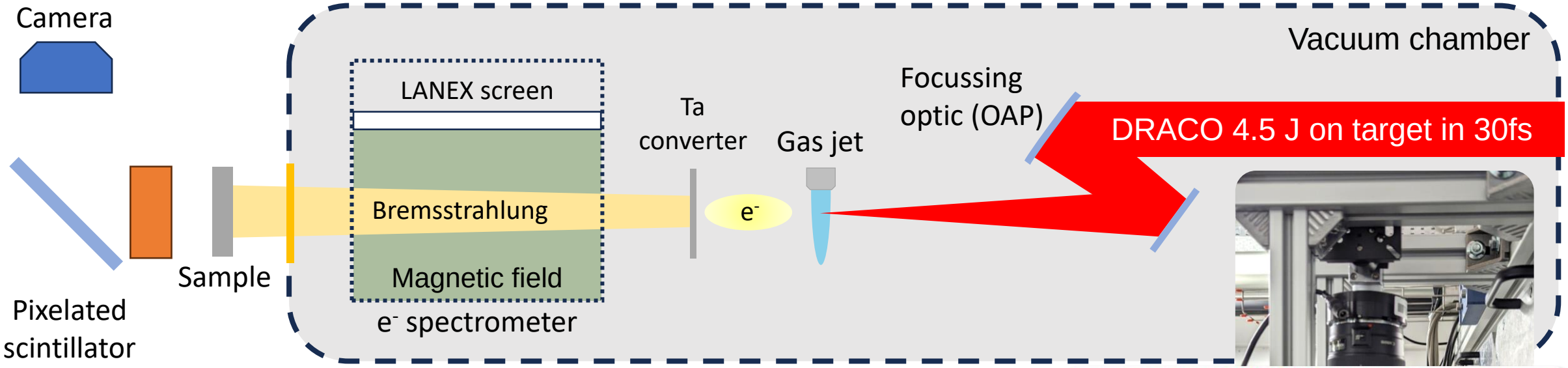

- Sample placed outside the chamber after a 125 µm Kapton window.
- Bremsstrahlung pointing measured online with a pixelated scintillator placed after the sample.

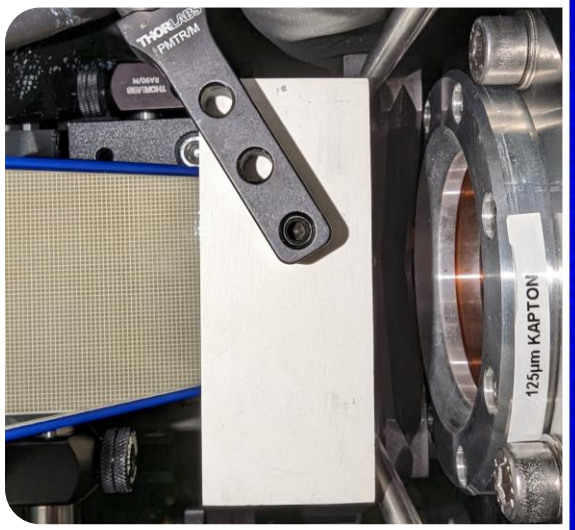

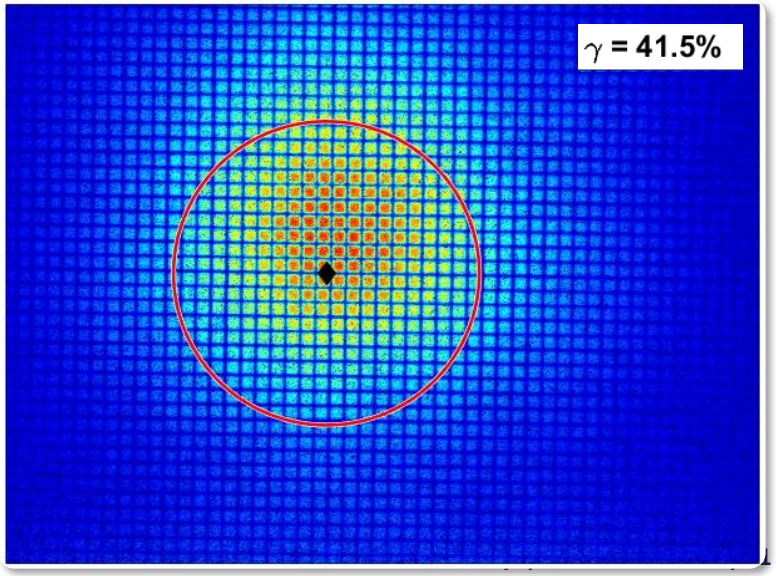

Demonstration of a photoreaction experiment

Case of interest

Multinucleon photonuclear reactions on ^{209}Bi: Experiment and evaluation

S.S. Belyshev[1], D.M. Filipescu[2], I. Gheoghe[2,3], B.S. Ishkhanov[1,4], V.V. Khankin[4], A.S. Kurilik[1], A.A. Kuznetsov[4], V.N. Orlin[4], N.N. Peskov[4], K.A. Stopani[4,a], O. Tesileanu[2], and V.V. Varlamov[4]

Abstract. Photon activation technique using bremsstrahlug with end-point energy 55.6 MeV is used to induce photonuclear reactions in a ^{209}Bi target. Absolute yields and integrated cross sections of multiparticle

Table 1. Experimental yields of photonuclear reactions on ^{209}Bi.

Reaction	Product	Yield, $10^{10} \times C^{-1}$
(γ, 5n1p)	^{203}Pb	73(7)
(γ, 6n)	^{203}Bi	7.8(7)

Case of interest

Multinucleon photonuclear reactions on ^{209}Bi: Experiment and evaluation

S.S. Belyshev[1], D.M. Filipescu[2], I. Gheoghe[2,3], B.S. Ishkhanov[1,4], V.V. Khankin[4], A.S. Kurilik[1], A.A. Kuznetsov[4], V.N. Orlin[4], N.N. Peskov[4], K.A. Stopani[4,a], O. Tesileanu[2], and V.V. Varlamov[4]

Abstract. Photon activation technique using bremsstrahlug with end-point energy 55.6 MeV is used to induce photonuclear reactions in a ^{209}Bi target. Absolute yields and integrated cross sections of multiparticle

Table 2. Comparison of the experimental yields of photonuclear reactions on ^{209}Bi with model calculations.

Reaction	$10^{10}\times$ Yield, C^{-1}		
	Experiment	CMPNR	TALYS
(γ, 5n1p)	73(7)	0.421	0.0148
(γ, 6n)	7.8(7)	0.399	6.29

Case of interest

Multinucleon photonuclear reactions on ^{209}Bi: Experiment and evaluation

S.S. Belyshev[1], D.M. Filipescu[2], I. Gheoghe[2,3], B.S. Ishkhanov[1,4], V.V. Khankin[4], A.S. Kurilik[1], A.A. Kuznetsov[4], V.N. Orlin[4], N.N. Peskov[4], K.A. Stopani[4,a], O. Tesileanu[2], and V.V. Varlamov[4]

Abstract. Photon activation technique using bremsstrahlug with end-point energy 55.6 MeV is used to induce photonuclear reactions in a ^{209}Bi target. Absolute yields and integrated cross sections of multiparticle

Belyshev, S.S. *et al.* (EPJ A, 2015)

Table 2. Comparison of the experimental yields of photonuclear reactions on ^{209}Bi with model calculations.

Reaction	$10^{10}\times$ Yield, C^{-1}		
	Experiment	CMPNR	TALYS
(γ, 5n1p)	73(7)	0.421	0.0148
(γ, 6n)	7.8(7)	0.399	6.29

Search for the evidence of ^{209}Bi(γ,p5n)^{203}Pb reaction in 60 MeV bremsstrahlung beams

M. Krmar[1,a], N. Jovančević[1], D. Maletić[2], Ž. Medić[2], D. Knežević[2], M. Savić[2], Yu. Teterev[3], S. Mitrofanov[3], K. D. Timoshenko[3], S. I. Alexeev[3], H. Marukyan[4], I. Kerobyan[4], R. Avetisyan[4], L. Poghosyan[4], R. Dallakyan[4], A. Hakobyan[4], L. Vahradyan[4], H. Mkrtchyan[4], A. Petrosyan[4]

M. Krmar *et al.* (EPJ A, 2023)

Table 2 Ratio p/q obtained using measured activities and simulation performed with six different models of level densities (in the same order as stated in Sect. 2.4)

	p/q ratio
Estimated using TALYS cross sections	0.00278
	0.0472
	0.000698
	0.0329
	0.5077
	0.0295
Estimated from Eq. 8	0.060(1)

Sample irradiation

- A ^{209}Bi sample of 25.4 mm × 2 mm was irradiated for 1 hour (370 shots).
- The sample was successfully activated and measured with a HPGe detector.
- Laser-plasma interaction creates an extremely harsh environment → HPGe detector must be in a different room (7 min transfer time).
- A short-lived activity of 10-100 Bq was measured.

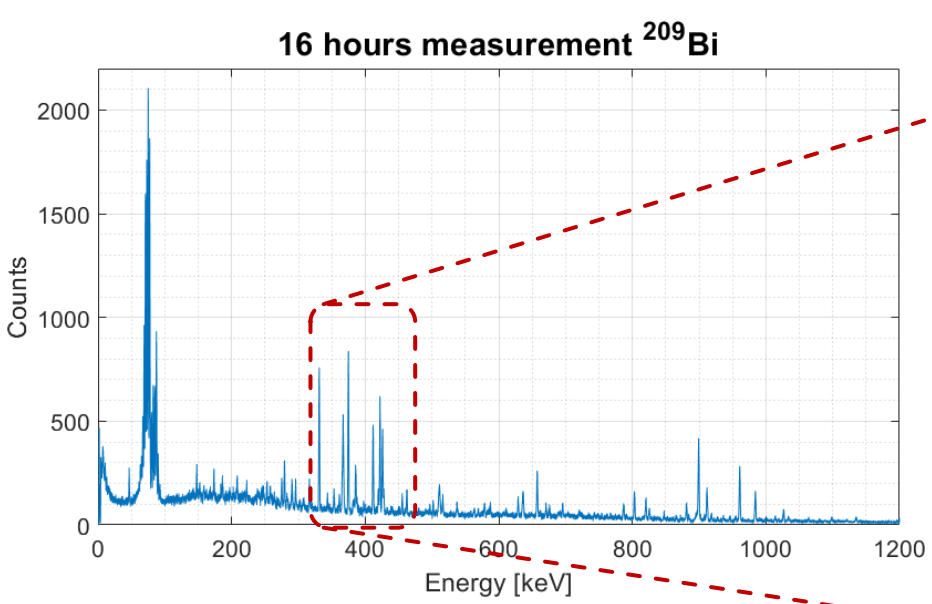

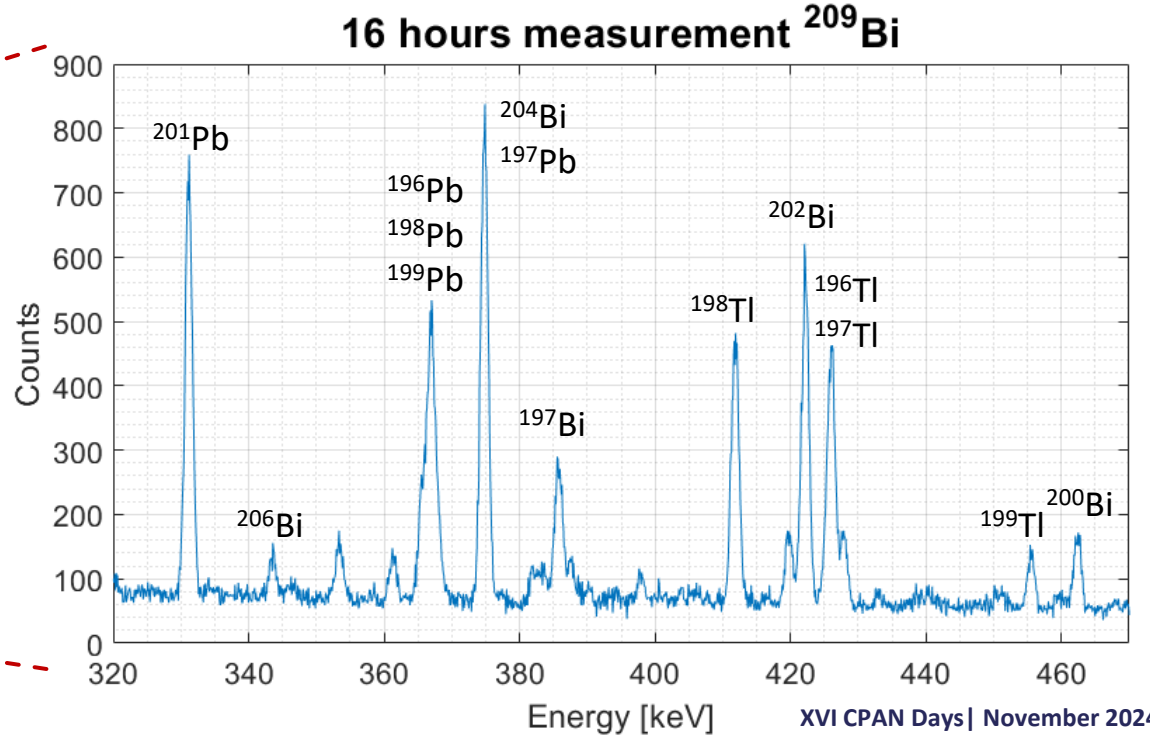

Generated bismuth isotopes

- Several Bi isotopes were identified using γ spectroscopy.

Region of interest of Chart of Nuclides

# Protons (Z) \ # Neutrons (N)	110	111	112	113	114	115	116	117	118	119	120	121	122	123	124	125	126
83	^{193}Bi 63.6 s	^{194}Bi 95 s	^{195}Bi 183 s	^{196}Bi 308 s	^{197}Bi 9.3 min	^{198}Bi 10 min	^{199}Bi 27 min	^{200}Bi 36 min	^{201}Bi 103 min	^{202}Bi 1.7 h	^{203}Bi 11.8 h	^{204}Bi 11.2 h	^{205}Bi 15.3 d	^{206}Bi 6.2 d	^{207}Bi 31.6 y	^{208}Bi 3.7e5 y	^{209}Bi stable
82	^{192}Pb 3.5 min	^{193}Pb 5.8 min	^{194}Pb 11 min	^{195}Pb 15 min	^{196}Pb 37 min	^{197}Pb 8.1 min	^{198}Pb 2.4 h	^{199}Pb 90 min	^{200}Pb 21.5 h	^{201}Pb 9.3 h	^{202}Pb 5.6e4 y	^{203}Pb 51.9 h	^{204}Pb stable	^{205}Pb 1.7e7 y	^{206}Pb stable	^{207}Pb stable	^{208}Pb stable
81	^{191}Tl 5.2 min	^{192}Tl 9.6 min	^{193}Tl 22 min	^{194}Tl 33 min	^{195}Tl 1.2 h	^{196}Tl 1.8 h	^{197}Tl 2.84 h	^{198}Tl 5.3 h	^{199}Tl 7.4 h	^{200}Tl 26.1 h	^{201}Tl 3.4 d	^{202}Tl 12.3 d	^{203}Tl stable	^{204}Tl 3.8 y	^{205}Tl stable	^{206}Tl 4.2 min	^{207}Tl 4.8 min
80	^{190}Hg 20 min	^{191}Hg 49 min	^{192}Hg 4.9 h	^{193}Hg 3.8 h	^{194}Hg 444 y	^{195}Hg 10.5 h	^{196}Hg stable	^{197}Hg 64.1 h	^{198}Hg stable	^{199}Hg stable	^{200}Hg stable	^{201}Hg stable	^{202}Hg stable	^{203}Hg 46.6 d	^{204}Hg stable	^{205}Hg 5.1 min	^{206}Hg 8.3 min

Generated bismuth isotopes

- Several Bi isotopes were identified using γ spectroscopy.

Region of interest of Chart of Nuclides

# Protons (Z) \ # Neutrons (N)	110	111	112	113	114	115	116	117	118	119	120	121	122	123	124	125	126
83	^{193}Bi 63.6 s	^{194}Bi 95 s	^{195}Bi 183 s	^{196}Bi 308 s	^{197}Bi 9.3 min	^{198}Bi 10 min	^{199}Bi 27 min	^{200}Bi 36 min	^{201}Bi 103 min	^{202}Bi 1.7 h	^{203}Bi 11.8 h	^{204}Bi 11.2 h	^{205}Bi 15.3 d	^{206}Bi 6.2 d	^{207}Bi 31.6 y	^{208}Bi 3.7e5 y	^{209}Bi stable
82	^{192}Pb 3.5 min	^{193}Pb 5.8 min	^{194}Pb 11 min	^{195}Pb 15 min	^{196}Pb 37 min	^{197}Pb 8.1 min	^{198}Pb 2.4 h	^{199}Pb 90 min	^{200}Pb 21.5 h	^{201}Pb 9.3 h	^{202}Pb 5.6e4 y	^{203}Pb 51.9 h	^{204}Pb stable	^{205}Pb 1.7e7 y	^{206}Pb stable	^{207}Pb stable	^{208}Pb stable
81	^{191}Tl 5.2 min	^{192}Tl 9.6 min	^{193}Tl 22 min	^{194}Tl 33 min	^{195}Tl 1.2 h	^{196}Tl 1.8 h	^{197}Tl 2.84 h	^{198}Tl 5.3 h	^{199}Tl 7.4 h	^{200}Tl 26.1 h	^{201}Tl 3.4 d	^{202}Tl 12.3 d	^{203}Tl stable	^{204}Tl 3.8 y	^{205}Tl stable	^{206}Tl 4.2 min	^{207}Tl 4.8 min
80	^{190}Hg 20 min	^{191}Hg 49 min	^{192}Hg 4.9 h	^{193}Hg 3.8 h	^{194}Hg 444 y	^{195}Hg 10.5 h	^{196}Hg stable	^{197}Hg 64.1 h	^{198}Hg stable	^{199}Hg stable	^{200}Hg stable	^{201}Hg stable	^{202}Hg stable	^{203}Hg 46.6 d	^{204}Hg stable	^{205}Hg 5.1 min	^{206}Hg 8.3 min

Generated bismuth isotopes

- Several Bi isotopes were identified using γ spectroscopy.

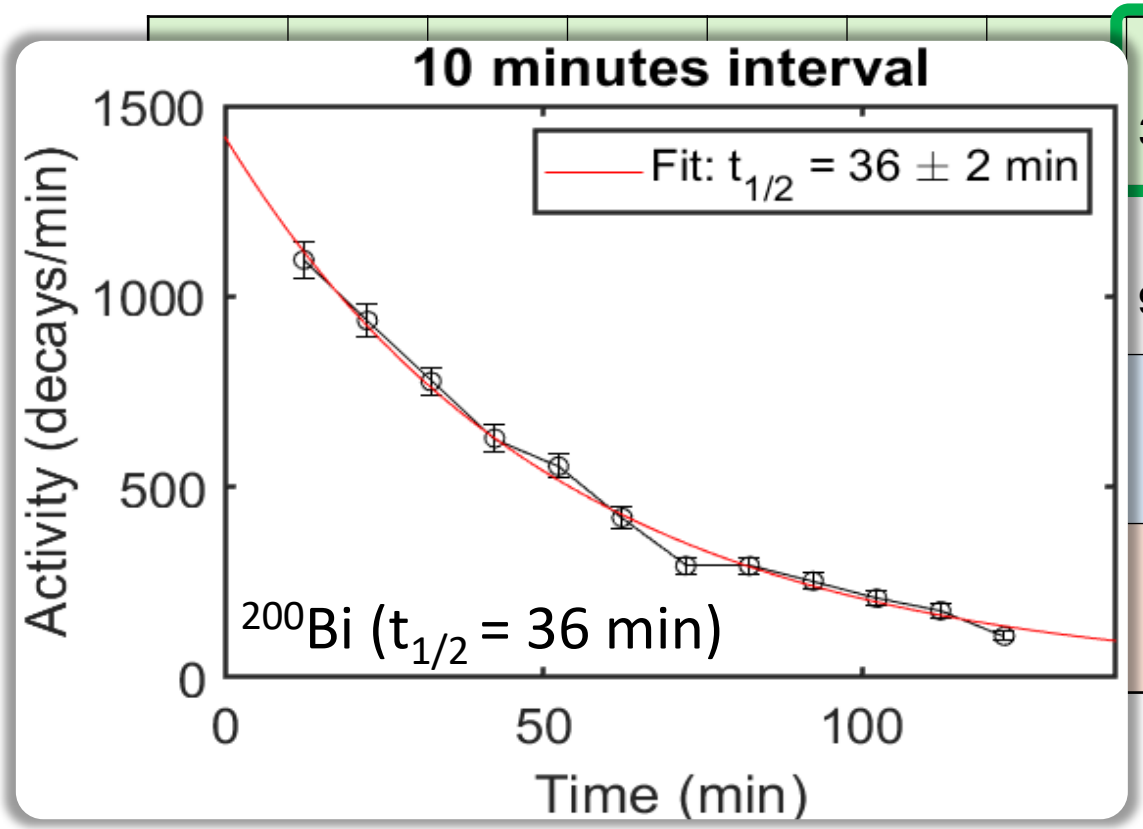

Region of interest of Chart of Nuclides

^{200}Bi 36 min	^{201}Bi 103 min	^{202}Bi 1.7 h	^{203}Bi 11.8 h	^{204}Bi 11.2 h	^{205}Bi 15.3 d	^{206}Bi 6.2 d	^{207}Bi 31.6 y	^{208}Bi 3.7e5 y	^{209}Bi stable
^{199}Pb 90 min	^{200}Pb 21.5 h	^{201}Pb 9.3 h	^{202}Pb 5.6e4 y	^{203}Pb 51.9 h	^{204}Pb stable	^{205}Pb 1.7e7 y	^{206}Pb stable	^{207}Pb stable	^{208}Pb stable
^{198}Tl 5.3 h	^{199}Tl 7.4 h	^{200}Tl 26.1 h	^{201}Tl 3.4 d	^{202}Tl 12.3 d	^{203}Tl stable	^{204}Tl 3.8 y	^{205}Tl stable	^{206}Tl 4.2 min	^{207}Tl 4.8 min
^{197}Hg 64.1 h	^{198}Hg stable	^{199}Hg stable	^{200}Hg stable	^{201}Hg stable	^{202}Hg stable	^{203}Hg 46.6 d	^{204}Hg stable	^{205}Hg 5.1 min	^{206}Hg 8.3 min
117	118	119	120	121	122	123	124	125	126

Neutrons (N)

Generated bismuth isotopes

- Several Bi isotopes were identified using γ spectroscopy.

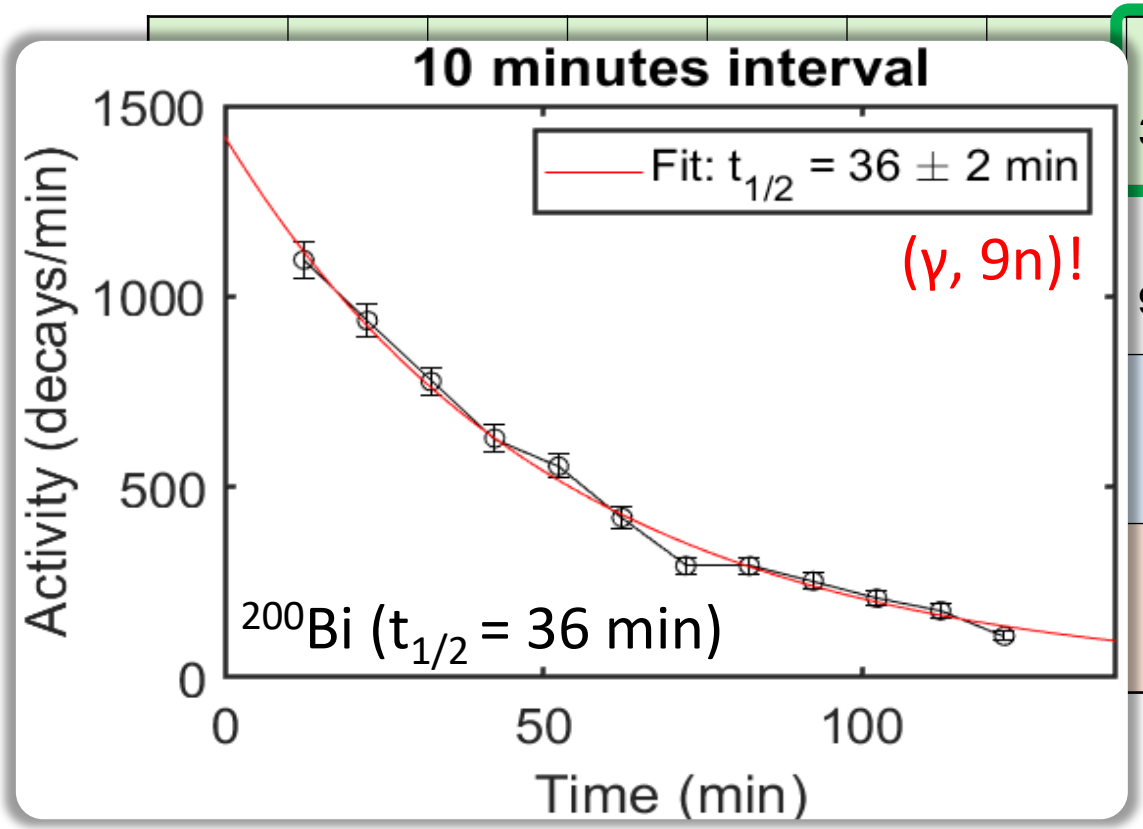

Region of interest of Chart of Nuclides

^{200}Bi 36 min	^{201}Bi 103 min	^{202}Bi 1.7 h	^{203}Bi 11.8 h	^{204}Bi 11.2 h	^{205}Bi 15.3 d	^{206}Bi 6.2 d	^{207}Bi 31.6 y	^{208}Bi 3.7e5 y	^{209}Bi stable
^{199}Pb 90 min	^{200}Pb 21.5 h	^{201}Pb 9.3 h	^{202}Pb 5.6e4 y	^{203}Pb 51.9 h	^{204}Pb stable	^{205}Pb 1.7e7 y	^{206}Pb stable	^{207}Pb stable	^{208}Pb stable
^{198}Tl 5.3 h	^{199}Tl 7.4 h	^{200}Tl 26.1 h	^{201}Tl 3.4 d	^{202}Tl 12.3 d	^{203}Tl stable	^{204}Tl 3.8 y	^{205}Tl stable	^{206}Tl 4.2 min	^{207}Tl 4.8 min
^{197}Hg 64.1 h	^{198}Hg stable	^{199}Hg stable	^{200}Hg stable	^{201}Hg stable	^{202}Hg stable	^{203}Hg 46.6 d	^{204}Hg stable	^{205}Hg 5.1 min	^{206}Hg 8.3 min
117	118	119	120	121	122	123	124	125	126

Neutrons (N)

Relative yields for bismuth

- Relative activations yields can be calculated for the identified Bi isotopes.

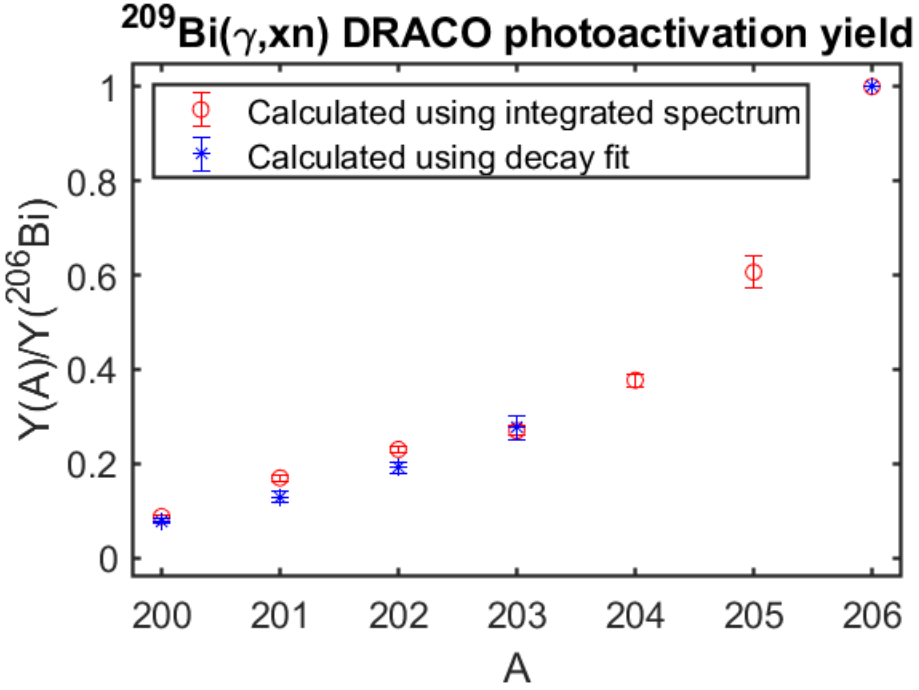

Relative yields for bismuth

- Relative activations yields can be calculated for the identified Bi isotopes.

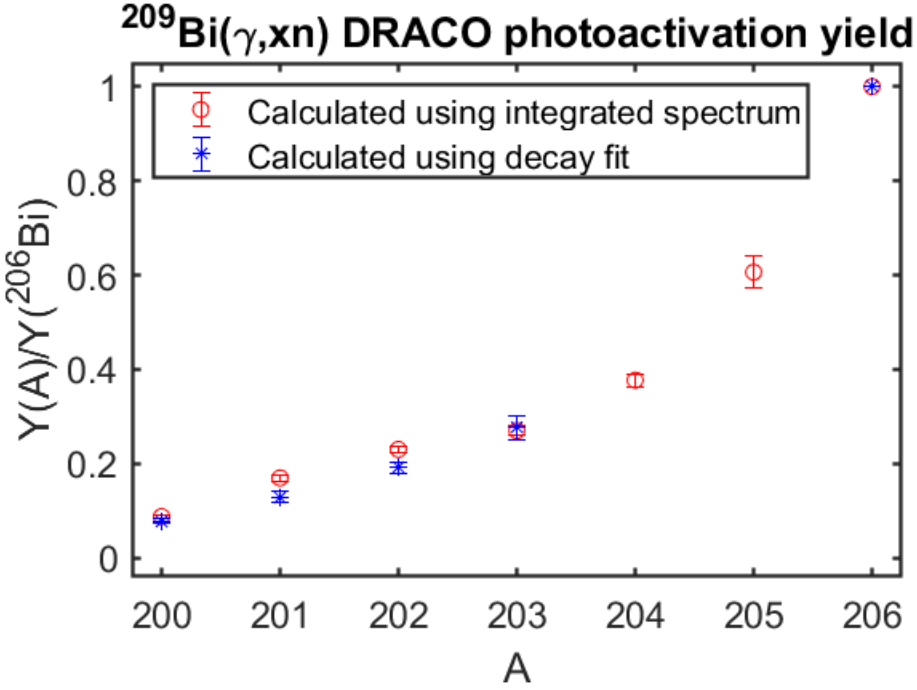

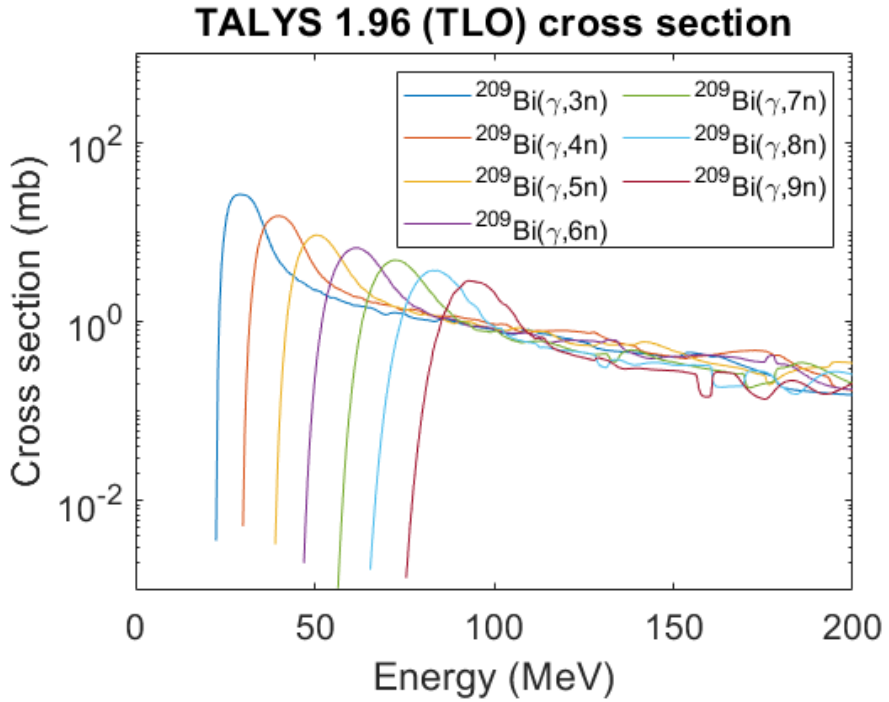

- We can compare with the numerical predictions using TALYS 1.96.

Relative yields for bismuth

- Relative activations yields can be calculated for the identified Bi isotopes.

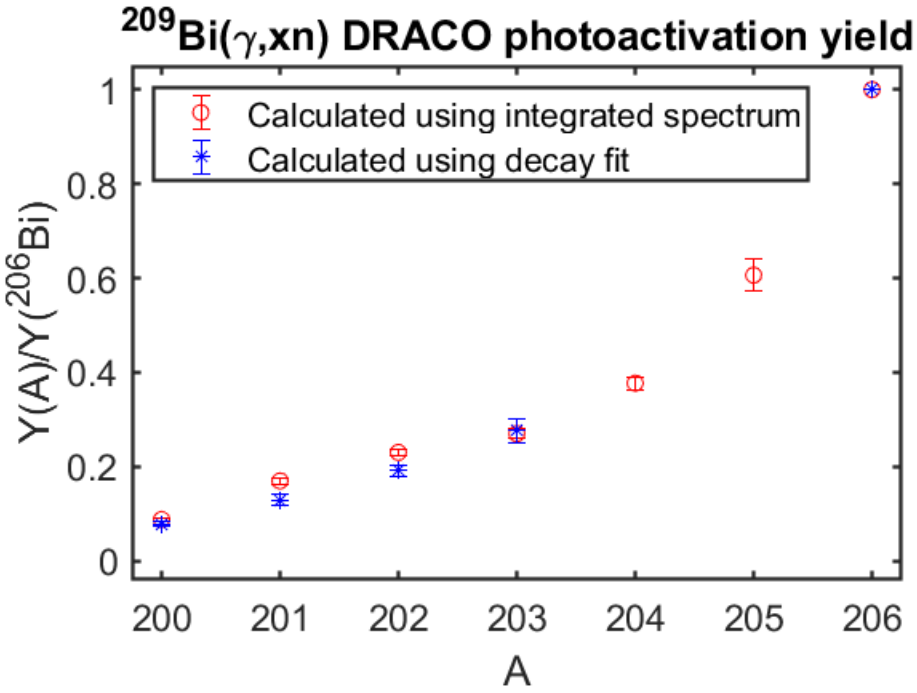

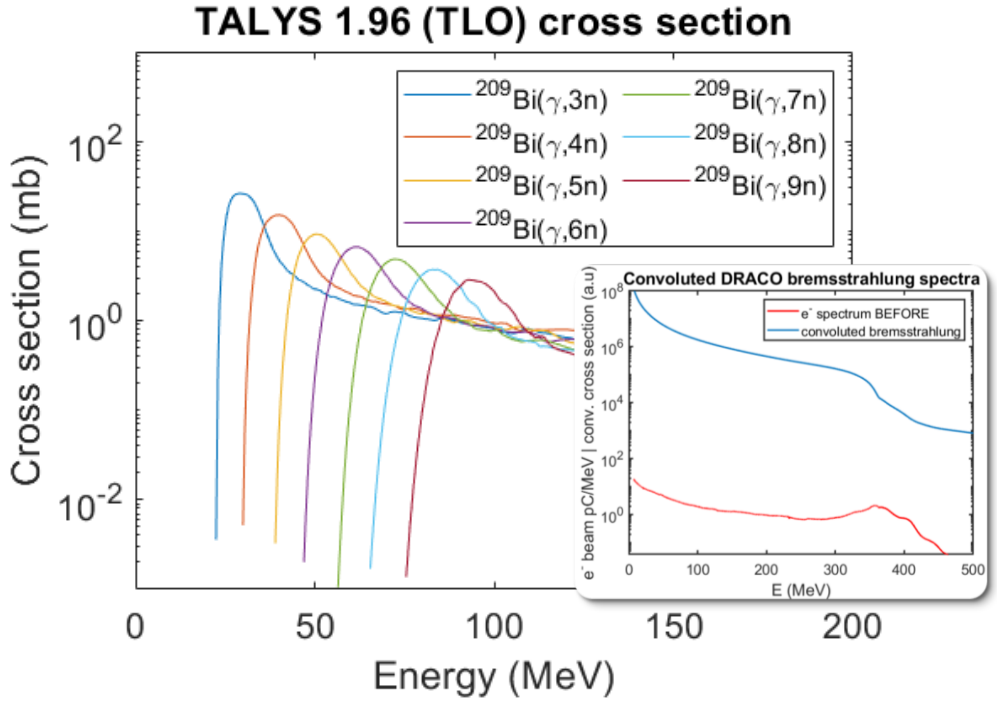

- We can compare with the numerical predictions using TALYS 1.96.

Relative yields for bismuth

- Relative activations yields can be calculated for the identified Bi isotopes.

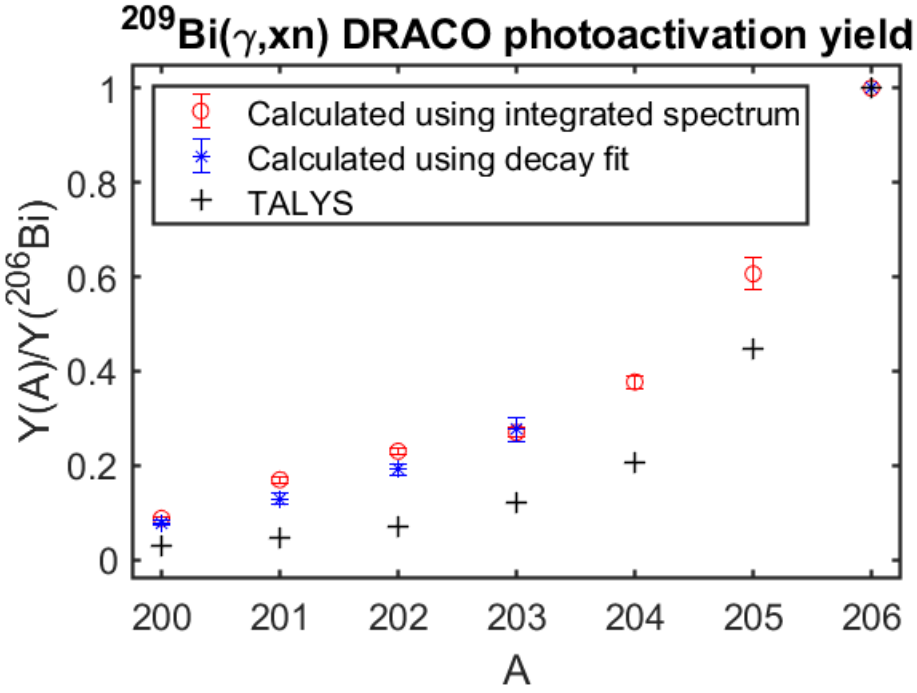

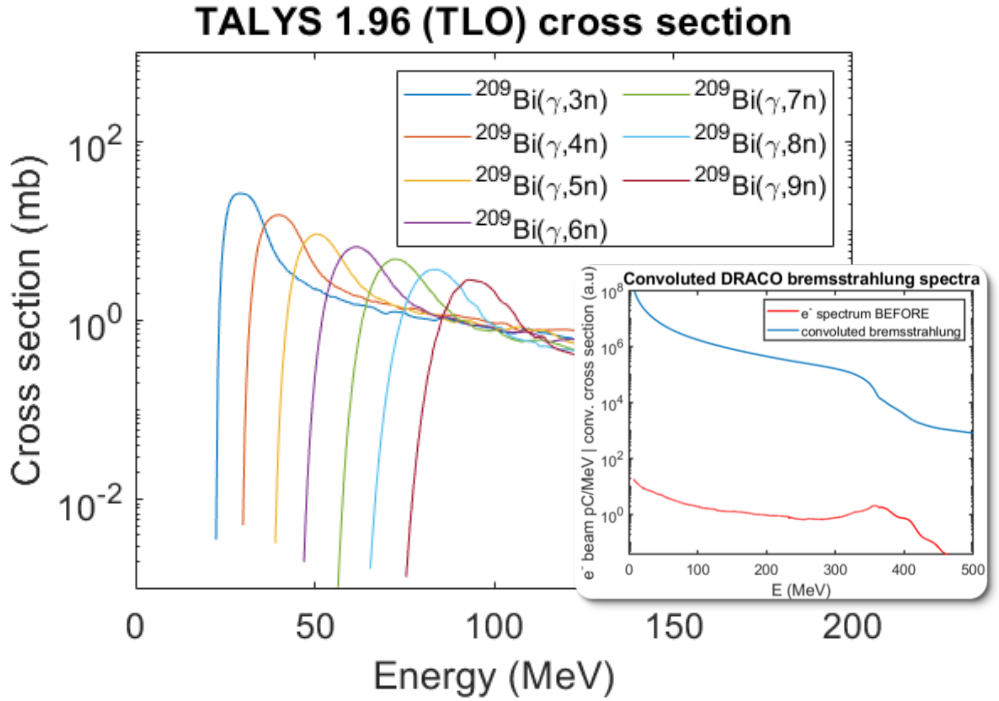

- We can compare with the numerical predictions using TALYS 1.96.
- Although the trend is reproduced, relative activation yields are not well estimated.

Lighter elements

- In addition to Bi, lighter elements were identified.

Region of interest of Chart of Nuclides

# Protons (Z) \ # Neutrons (N)	110	111	112	113	114	115	116	117	118	119	120	121	122	123	124	125	126
83	^{193}Bi 63.6 s	^{194}Bi 95 s	^{195}Bi 183 s	^{196}Bi 308 s	^{197}Bi 9.3 min	^{198}Bi 10 min	^{199}Bi 27 min	^{200}Bi 36 min	^{201}Bi 103 min	^{202}Bi 1.7 h	^{203}Bi 11.8 h	^{204}Bi 11.2 h	^{205}Bi 15.3 d	^{206}Bi 6.2 d	^{207}Bi 31.6 y	^{208}Bi 3.7e5 y	^{209}Bi stable
82	^{192}Pb 3.5 min	^{193}Pb 5.8 min	^{194}Pb 11 min	^{195}Pb 15 min	^{196}Pb 37 min	^{197}Pb 8.1 min	^{198}Pb 2.4 h	^{199}Pb 90 min	^{200}Pb 21.5 h	^{201}Pb 9.3 h	^{202}Pb 5.6e4 y	^{203}Pb 51.9 h	^{204}Pb stable	^{205}Pb 1.7e7 y	^{206}Pb stable	^{207}Pb stable	^{208}Pb stable
81	^{191}Tl 5.2 min	^{192}Tl 9.6 min	^{193}Tl 22 min	^{194}Tl 33 min	^{195}Tl 1.2 h	^{196}Tl 1.8 h	^{197}Tl 2.84 h	^{198}Tl 5.3 h	^{199}Tl 7.4 h	^{200}Tl 26.1 h	^{201}Tl 3.4 d	^{202}Tl 12.3 d	^{203}Tl stable	^{204}Tl 3.8 y	^{205}Tl stable	^{206}Tl 4.2 min	^{207}Tl 4.8 min
80	^{190}Hg 20 min	^{191}Hg 49 min	^{192}Hg 4.9 h	^{193}Hg 3.8 h	^{194}Hg 444 y	^{195}Hg 10.5 h	^{196}Hg stable	^{197}Hg 64.1 h	^{198}Hg stable	^{199}Hg stable	^{200}Hg stable	^{201}Hg stable	^{202}Hg stable	^{203}Hg 46.6 d	^{204}Hg stable	^{205}Hg 5.1 min	^{206}Hg 8.3 min

Lighter elements

- In addition to Bi, lighter elements were identified.

Region of interest of Chart of Nuclides

# Protons (Z) \ # Neutrons (N)	110	111	112	113	114	115	116	117	118	119	120	121	122	123	124	125	126
83	^{193}Bi 63.6 s	^{194}Bi 95 s	^{195}Bi 183 s	^{196}Bi 308 s	^{197}Bi 9.3 min	^{198}Bi 10 min	^{199}Bi 27 min	^{200}Bi 36 min	^{201}Bi 103 min	^{202}Bi 1.7 h	^{203}Bi 11.8 h	^{204}Bi 11.2 h	^{205}Bi 15.3 d	^{206}Bi 6.2 d	^{207}Bi 31.6 y	^{208}Bi 3.7e5 y	^{209}Bi stable
82	^{192}Pb 3.5 min	^{193}Pb 5.8 min	^{194}Pb 11 min	^{195}Pb 15 min	^{196}Pb 37 min	^{197}Pb 8.1 min	^{198}Pb 2.4 h	^{199}Pb 90 min	^{200}Pb 21.5 h	^{201}Pb 9.3 h	^{202}Pb 5.6e4 y	^{203}Pb 51.9 h	^{204}Pb stable	^{205}Pb 1.7e7 y	^{206}Pb stable	^{207}Pb stable	^{208}Pb stable
81	^{191}Tl 5.2 min	^{192}Tl 9.6 min	^{193}Tl 22 min	^{194}Tl 33 min	^{195}Tl 1.2 h	^{196}Tl 1.8 h	^{197}Tl 2.84 h	^{198}Tl 5.3 h	^{199}Tl 7.4 h	^{200}Tl 26.1 h	^{201}Tl 3.4 d	^{202}Tl 12.3 d	^{203}Tl stable	^{204}Tl 3.8 y	^{205}Tl stable	^{206}Tl 4.2 min	^{207}Tl 4.8 min
80	^{190}Hg 20 min	^{191}Hg 49 min	^{192}Hg 4.9 h	^{193}Hg 3.8 h	^{194}Hg 444 y	^{195}Hg 10.5 h	^{196}Hg stable	^{197}Hg 64.1 h	^{198}Hg stable	^{199}Hg stable	^{200}Hg stable	^{201}Hg stable	^{202}Hg stable	^{203}Hg 46.6 d	^{204}Hg stable	^{205}Hg 5.1 min	^{206}Hg 8.3 min

Lighter elements

- In addition to Bi, lighter elements were identified.

Region of interest of Chart of Nuclides

# Protons (Z) \ # Neutrons (N)	110	111	112	113	114	115	116	117	118	119	120
83	^{193}Bi 63.6 s	^{194}Bi 95 s	^{195}Bi 183 s	^{196}Bi 308 s	^{197}Bi 9.3 min	^{198}Bi 10 min	^{199}Bi 27 min	^{200}Bi 36 min	^{201}Bi 103 min	^{202}Bi 1.7 h	^{203}Bi 11.8 h
82	^{192}Pb 3.5 min	^{193}Pb 5.8 min	^{194}Pb 11 min	^{195}Pb 15 min	^{196}Pb 37 min	^{197}Pb 8.1 min	^{198}Pb 2.4 h	^{199}Pb 90 min	^{200}Pb 21.5 h	^{201}Pb 9.3 h	^{202}Pb 5.6e4 y
81	^{191}Tl 5.2 min	^{192}Tl 9.6 min	^{193}Tl 22 min	^{194}Tl 33 min	^{195}Tl 1.2 h	^{196}Tl 1.8 h	^{197}Tl 2.84 h	^{198}Tl 5.3 h	^{199}Tl 7.4 h	^{200}Tl 26.1 h	^{201}Tl 3.4 d
80	^{190}Hg 20 min	^{191}Hg 49 min	^{192}Hg 4.9 h	^{193}Hg 3.8 h	^{194}Hg 444 y	^{195}Hg 10.5 h	^{196}Hg stable	^{197}Hg 64.1 h	^{198}Hg stable	^{199}Hg stable	^{200}Hg stable

# Protons (Z) \ # Neutrons (N)	120	121	122	123	124	125	126
83	^{203}Bi 11.8 h	^{204}Bi 11.2 h	^{205}Bi 15.3 d	^{206}Bi 6.2 d	^{207}Bi 31.6 y	^{208}Bi 3.7e5 y	^{209}Bi stable
82	^{202}Pb 5.6e4 y	^{203}Pb 51.9 h	^{204}Pb stable	^{205}Pb 1.7e7 y	^{206}Pb stable	^{207}Pb stable	^{208}Pb stable
81	^{201}Tl 3.4 d	^{202}Tl 12.3 d	^{203}Tl stable	^{204}Tl 3.8 y	^{205}Tl stable	^{206}Tl 4.2 min	^{207}Tl 4.8 min
80	^{200}Hg stable	^{201}Hg stable	^{202}Hg stable	^{203}Hg 46.6 d	^{204}Hg stable	^{205}Hg 5.1 min	^{206}Hg 8.3 min

Where do they come from?

Lighter elements

- In addition to Bi, lighter elements were identified.

Region of interest of Chart of Nuclides

# Protons (Z) \ # Neutrons (N)	110	111	112	113	114	115	116	117	118	119	120
83	^{193}Bi 63.6 s	^{194}Bi 95 s	^{195}Bi 183 s	^{196}Bi 308 s	^{197}Bi 9.3 min	^{198}Bi 10 min	^{199}Bi 27 min	^{200}Bi 36 min	^{201}Bi 103 min	^{202}Bi 1.7 h	^{203}Bi 11.8 h
82	^{192}Pb 3.5 min	^{193}Pb 5.8 min	^{194}Pb 11 min	^{195}Pb 15 min	^{196}Pb 37 min	^{197}Pb 8.1 min	^{198}Pb 2.4 h	^{199}Pb 90 min	^{200}Pb 21.5 h	^{201}Pb 9.3 h	^{202}Pb 5.6e4 y
81	^{191}Tl 5.2 min	^{192}Tl 9.6 min	^{193}Tl 22 min	^{194}Tl 33 min	^{195}Tl 1.2 h	^{196}Tl 1.8 h	^{197}Tl 2.84 h	^{198}Tl 5.3 h	^{199}Tl 7.4 h	^{200}Tl 26.1 h	^{201}Tl 3.4 d
80	^{190}Hg 20 min	^{191}Hg 49 min	^{192}Hg 4.9 h	^{193}Hg 3.8 h	^{194}Hg 444 y	^{195}Hg 10.5 h	^{196}Hg stable	^{197}Hg 64.1 h	^{198}Hg stable	^{199}Hg stable	^{200}Hg stable

# Protons (Z) \ # Neutrons (N)	120	121	122	123	124	125	126
83	^{203}Bi 11.8 h	^{204}Bi 11.2 h	^{205}Bi 15.3 d	^{206}Bi 6.2 d	^{207}Bi 31.6 y	^{208}Bi 3.7e5 y	^{209}Bi stable
82	^{202}Pb 5.6e4 y	^{203}Pb 51.9 h	^{204}Pb stable	^{205}Pb 1.7e7 y	^{206}Pb stable	^{207}Pb stable	^{208}Pb stable
81	^{201}Tl 3.4 d	^{202}Tl 12.3 d	^{203}Tl stable	^{204}Tl 3.8 y	^{205}Tl stable	^{206}Tl 4.2 min	^{207}Tl 4.8 min
80	^{200}Hg stable	^{201}Hg stable	^{202}Hg stable	^{203}Hg 46.6 d	^{204}Hg stable	^{205}Hg 5.1 min	^{206}Hg 8.3 min

Where do they come from?

Lead generation

- These isotopes could come from the Bi decay chain (^{203}Pb for example)

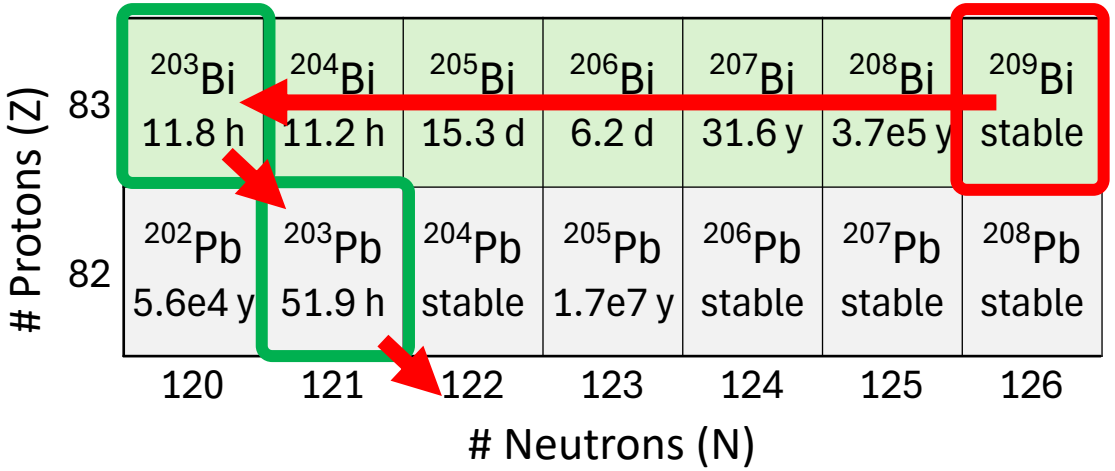

$$\frac{dN_{Pb}}{dt} = \lambda_{Bi} N_{Bi} - \lambda_{Pb} N_{Pb}$$

$$\frac{N_{Pb}(t_0)}{N_{Bi}(t_0)} = \frac{\frac{\lambda_{Bi}}{\lambda_{Pb}}\left(1 - e^{-\lambda_{Pb} t_{irr}}\right) + \frac{\lambda_{Bi}}{\lambda_{Pb} - \lambda_{Bi}}\left(e^{-\lambda_{Pb} t_{irr}} - e^{-\lambda_{Bi} t_{irr}}\right)}{1 - e^{-\lambda_{Bi} t_{irr}}}$$

At the begining of the decay, t_0, the ratio is estimated depending on the irradiation time t_{irr}.

Lead generation

- These isotopes could come from the Bi decay chain (^{203}Pb for example)

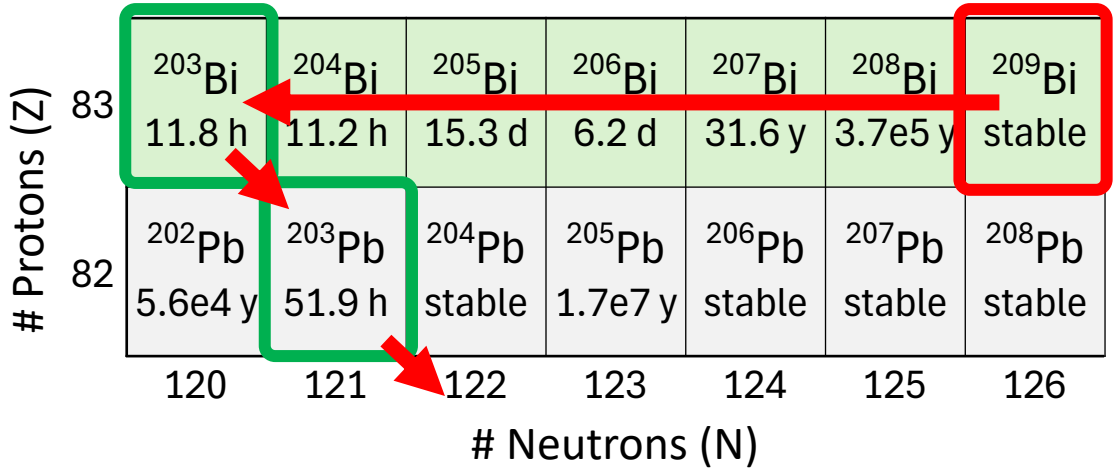

$$\frac{dN_{Pb}}{dt} = \lambda_{Bi}N_{Bi} - \lambda_{Pb}N_{Pb}$$

$$\frac{N_{Pb}(t_0)}{N_{Bi}(t_0)} = \frac{\frac{\lambda_{Bi}}{\lambda_{Pb}}\left(1 - e^{-\lambda_{Pb}t_{irr}}\right) + \frac{\lambda_{Bi}}{\lambda_{Pb} - \lambda_{Bi}}\left(e^{-\lambda_{Pb}t_{irr}} - e^{-\lambda_{Bi}t_{irr}}\right)}{1 - e^{-\lambda_{Bi}t_{irr}}}$$

At the begining of the decay, t_0, the ratio is estimated depending on the irradiation time t_{irr}.

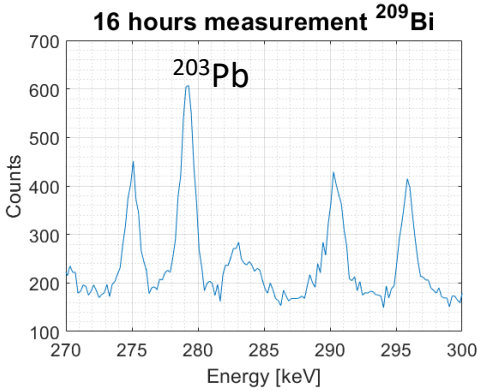

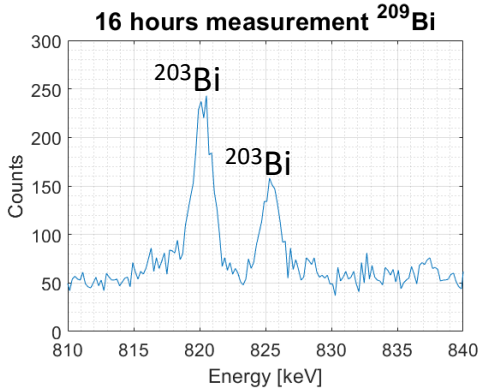

Theoretical ratio of ^{203}Pb produced by the decay of ^{203}Bi:

t_0 ≡ time of irradiation (60.67 min)

$$\frac{N_{Pb}^{Th}(t_0)}{N_{Bi}^{Th}(t_0)} = 0.030$$

Experimental ratio:
(From integrated counts)

$$\frac{N_{Pb}^{Exp}(t_0)}{N_{Bi}^{Exp}(t_0)} = 0.642$$

Lead generation

- These isotopes could come from the Bi decay chain (^{203}Pb for example)

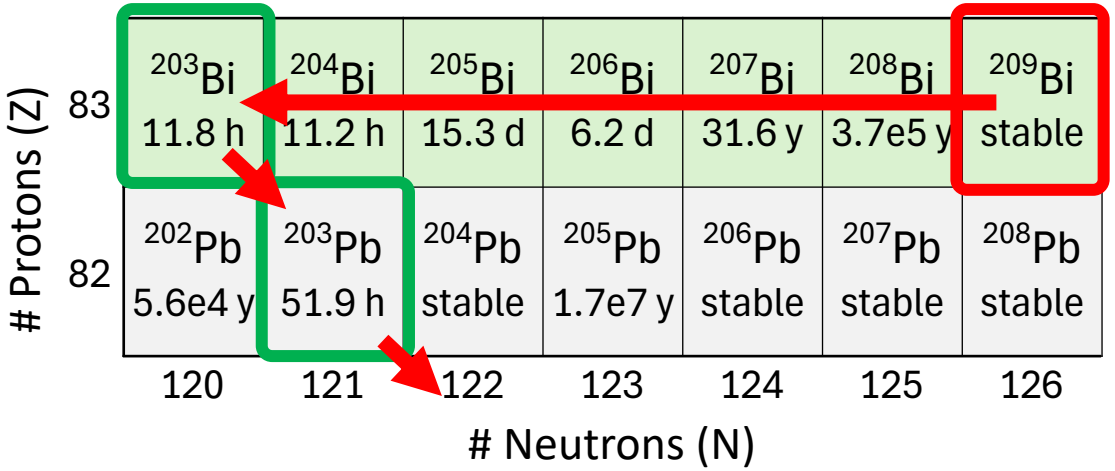

$$\frac{dN_{Pb}}{dt} = \lambda_{Bi}N_{Bi} - \lambda_{Pb}N_{Pb}$$

$$\frac{N_{Pb}(t_0)}{N_{Bi}(t_0)} = \frac{\frac{\lambda_{Bi}}{\lambda_{Pb}}\left(1 - e^{-\lambda_{Pb}t_{irr}}\right) + \frac{\lambda_{Bi}}{\lambda_{Pb} - \lambda_{Bi}}\left(e^{-\lambda_{Pb}t_{irr}} - e^{-\lambda_{Bi}t_{irr}}\right)}{1 - e^{-\lambda_{Bi}t_{irr}}}$$

At the begining of the decay, t_0, the ratio is estimated depending on the irradiation time t_{irr}.

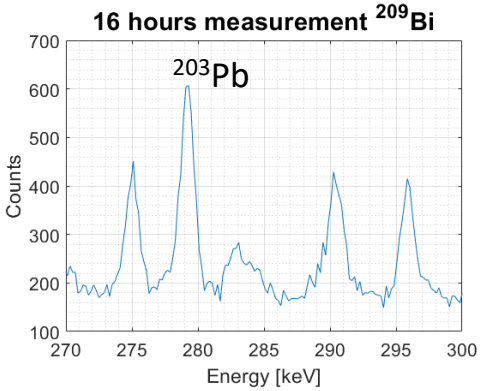

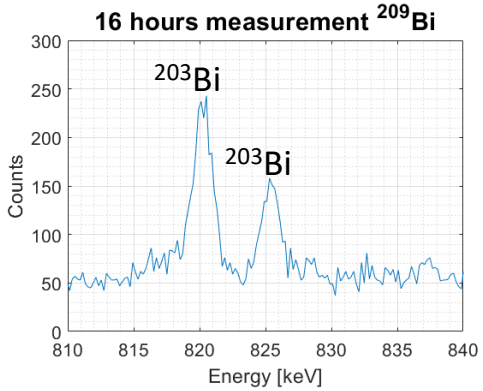

Theoretical ratio of ^{203}Pb produced by the decay of ^{203}Bi:

t_0 ≡ time of irradiation (60.67 min)

$$\frac{N_{Pb}^{Th}(t_0)}{N_{Bi}^{Th}(t_0)} = 0.030$$

Experimental ratio:
(From integrated counts)

$$\frac{N_{Pb}^{Exp}(t_0)}{N_{Bi}^{Exp}(t_0)} = 0.642$$

✗ Not all Pb can come from Bi decay!

Lead generation

- Direct production of ^{203}Pb must be taking place, ^{209}Bi(γ,p5n)^{203}Pb.

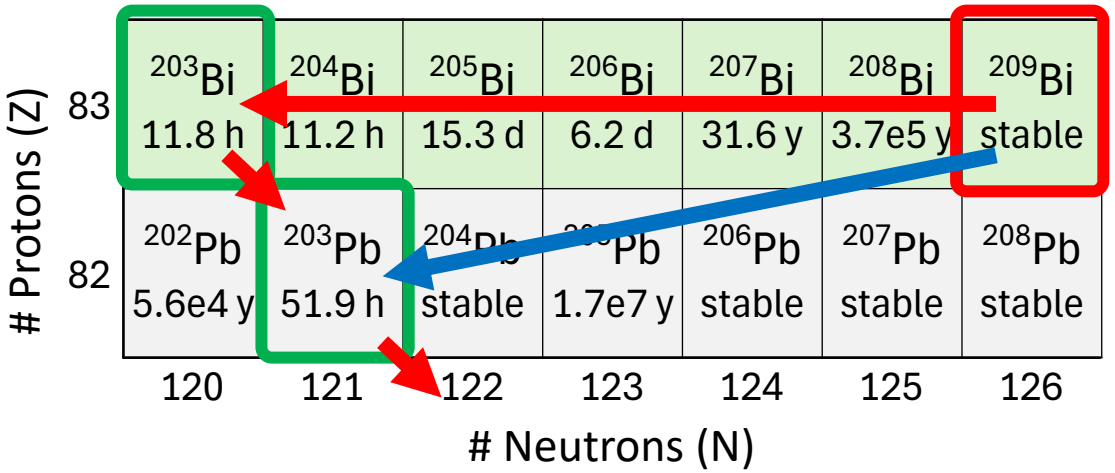

$$\frac{dN_{Pb}}{dt} = \lambda_{Bi}N_{Bi} + p - \lambda_{Pb}N_{Pb}$$

$p \equiv$ direct production rate of ^{203}Pb

$q \equiv$ direct production rate of ^{203}Bi

$$\frac{N_{Pb}(t_0)}{N_{Bi}(t_0)} = \frac{\left(1 + \frac{p}{q}\right)\frac{\lambda_{Bi}}{\lambda_{Pb}}\left(1 - e^{-\lambda_{Pb}t_{irr}}\right) + \frac{\lambda_{Bi}}{\lambda_{Pb} - \lambda_{Bi}}\left(e^{-\lambda_{Pb}t_{irr}} - e^{-\lambda_{Bi}t_{irr}}\right)}{1 - e^{-\lambda_{Bi}t_{irr}}}$$

M. Krmar *et al.* (EPJ A, 2023)

Lead generation

- Direct production of ^{203}Pb must be taking place, ^{209}Bi(γ,p5n)^{203}Pb.

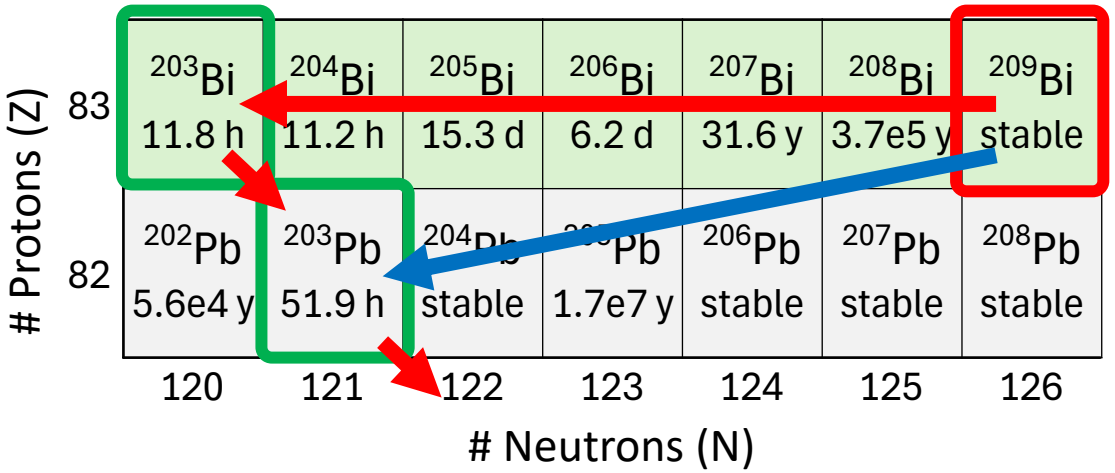

$$\frac{dN_{Pb}}{dt} = \lambda_{Bi}N_{Bi} + p - \lambda_{Pb}N_{Pb}$$

$p \equiv$ direct production rate of ^{203}Pb

$q \equiv$ direct production rate of ^{203}Bi

$$\frac{N_{Pb}(t_0)}{N_{Bi}(t_0)} = \frac{\left(1+\frac{p}{q}\right)\frac{\lambda_{Bi}}{\lambda_{Pb}}\left(1-e^{-\lambda_{Pb}t_{irr}}\right) + \frac{\lambda_{Bi}}{\lambda_{Pb}-\lambda_{Bi}}\left(e^{-\lambda_{Pb}t_{irr}} - e^{-\lambda_{Bi}t_{irr}}\right)}{1-e^{-\lambda_{Bi}t_{irr}}}$$

M. Krmar *et al.* (EPJ A, 2023)

- <u>Method 1</u>: Analytical.

$$\frac{N_{Pb}^{Exp}(t_0)}{N_{Bi}^{Exp}(t_0)} = \left[\frac{N_{Pb}^{Exp}}{N_{Bi}^{Exp}} - \frac{\lambda_{Bi}}{\lambda_{Bi}-\lambda_{Pb}}\frac{e^{-\lambda_{Pb}t_1} - e^{-\lambda_{Pb}t_2}}{e^{-\lambda_{Bi}t_1} - e^{-\lambda_{Bi}t_2}} + \frac{\lambda_{Pb}}{\lambda_{Bi}-\lambda_{Pb}}\right]\frac{e^{-\lambda_{Bi}t_1} - e^{-\lambda_{Bi}t_2}}{e^{-\lambda_{Pb}t_1} - e^{-\lambda_{Pb}t_2}}$$

Lead generation

- Direct production of ^{203}Pb must be taking place, ^{209}Bi(γ,p5n)^{203}Pb.

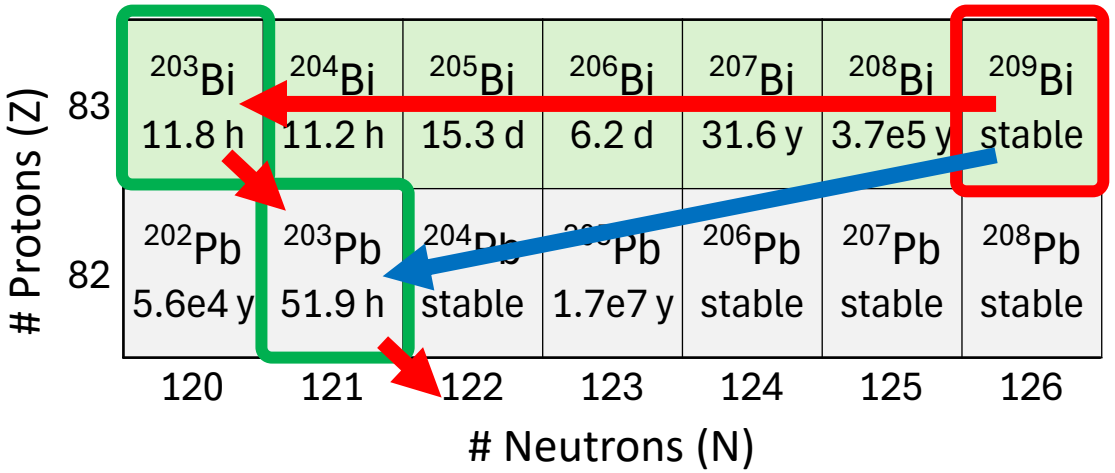

$$\frac{dN_{Pb}}{dt} = \lambda_{Bi}N_{Bi} + p - \lambda_{Pb}N_{Pb}$$

$p \equiv$ direct production rate of ^{203}Pb

$q \equiv$ direct production rate of ^{203}Bi

$$\frac{N_{Pb}(t_0)}{N_{Bi}(t_0)} = \frac{\left(1+\frac{p}{q}\right)\frac{\lambda_{Bi}}{\lambda_{Pb}}\left(1-e^{-\lambda_{Pb}t_{irr}}\right) + \frac{\lambda_{Bi}}{\lambda_{Pb}-\lambda_{Bi}}\left(e^{-\lambda_{Pb}t_{irr}} - e^{-\lambda_{Bi}t_{irr}}\right)}{1-e^{-\lambda_{Bi}t_{irr}}}$$

M. Krmar *et al.* (EPJ A, 2023)

- <u>Method 1</u>: Analytical.

$$\frac{N_{Pb}^{Exp}(t_0)}{N_{Bi}^{Exp}(t_0)} = \left[\frac{N_{Pb}^{Exp}}{N_{Bi}^{Exp}} - \frac{\lambda_{Bi}}{\lambda_{Bi}-\lambda_{Pb}}\frac{e^{-\lambda_{Pb}t_1}-e^{-\lambda_{Pb}t_2}}{e^{-\lambda_{Bi}t_1}-e^{-\lambda_{Bi}t_2}} + \frac{\lambda_{Pb}}{\lambda_{Bi}-\lambda_{Pb}}\right]\frac{e^{-\lambda_{Bi}t_1}-e^{-\lambda_{Bi}t_2}}{e^{-\lambda_{Pb}t_1}-e^{-\lambda_{Pb}t_2}}$$

- <u>Method 2</u>: Temporal decay fit.

$$A_{Pb} = \frac{\lambda_{Bi}\lambda_{Pb}}{\lambda_{Pb}-\lambda_{Bi}}N_0^{Bi}\left[e^{-\lambda_{Bi}t} - e^{-\lambda_{Pb}t}\right] + \lambda_{Pb}N_0^{Pb}e^{-\lambda_{Pb}t}$$

Lead generation

- Direct production of ^{203}Pb must be taking place, ^{209}Bi(γ,p5n)^{203}Pb.

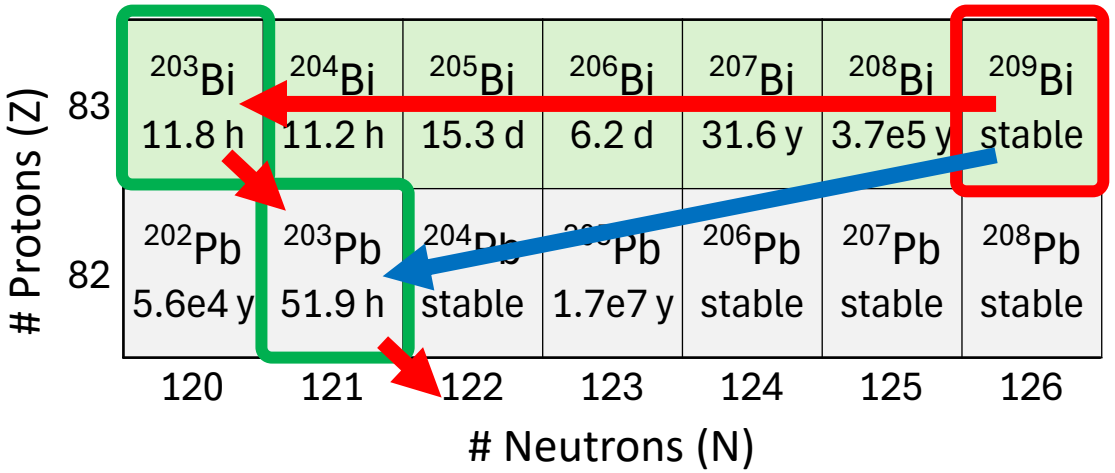

$$\frac{dN_{Pb}}{dt} = \lambda_{Bi}N_{Bi} + p - \lambda_{Pb}N_{Pb}$$

$p \equiv$ direct production rate of ^{203}Pb

$q \equiv$ direct production rate of ^{203}Bi

$$\frac{N_{Pb}(t_0)}{N_{Bi}(t_0)} = \frac{\left(1+\frac{p}{q}\right)\frac{\lambda_{Bi}}{\lambda_{Pb}}\left(1-e^{-\lambda_{Pb}t_{irr}}\right) + \frac{\lambda_{Bi}}{\lambda_{Pb}-\lambda_{Bi}}\left(e^{-\lambda_{Pb}t_{irr}} - e^{-\lambda_{Bi}t_{irr}}\right)}{1-e^{-\lambda_{Bi}t_{irr}}}$$

M. Krmar *et al.* (EPJ A, 2023)

- Method 1: Analytical.

$$\frac{N_{Pb}^{Exp}(t_0)}{N_{Bi}^{Exp}(t_0)} = \left[\frac{N_{Pb}^{Exp}}{N_{Bi}^{Exp}} - \frac{\lambda_{Bi}}{\lambda_{Bi}-\lambda_{Pb}}\frac{e^{-\lambda_{Pb}t_1}-e^{-\lambda_{Pb}t_2}}{e^{-\lambda_{Bi}t_1}-e^{-\lambda_{Bi}t_2}} + \frac{\lambda_{Pb}}{\lambda_{Bi}-\lambda_{Pb}}\right]\frac{e^{-\lambda_{Bi}t_1}-e^{-\lambda_{Bi}t_2}}{e^{-\lambda_{Pb}t_1}-e^{-\lambda_{Pb}t_2}}$$

- Method 2: Temporal decay fit.

$$A_{Pb} = \frac{\lambda_{Bi}\lambda_{}}{\lambda_{Pb}-} \quad \text{…} \; e^{-\lambda_{Pb}t}$$

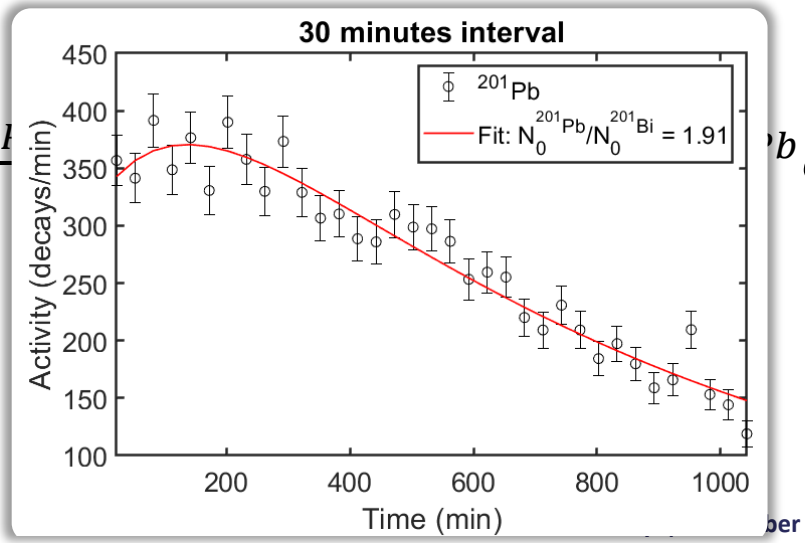

Yields of lighter elements

- The relative yields of Pb can be calculated using the same procedure as for Bi.

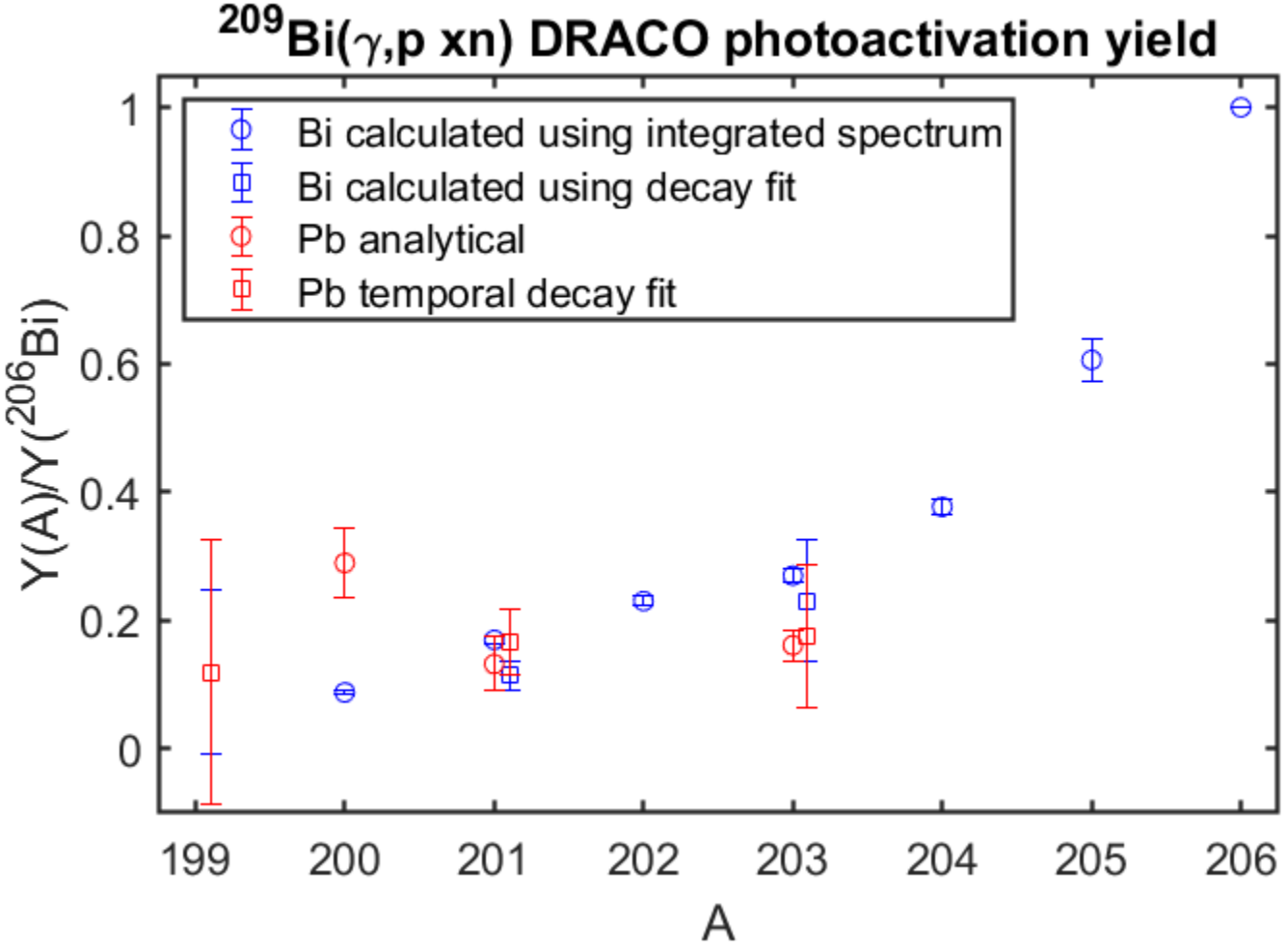

Yields of lighter elements

- The relative yields of Pb can be calculated using the same procedure as for Bi.
- TALYS simulations don't reproduce experiment.

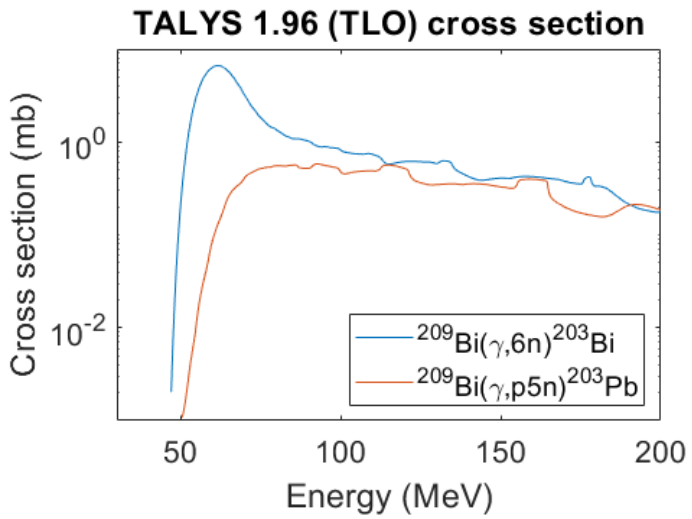

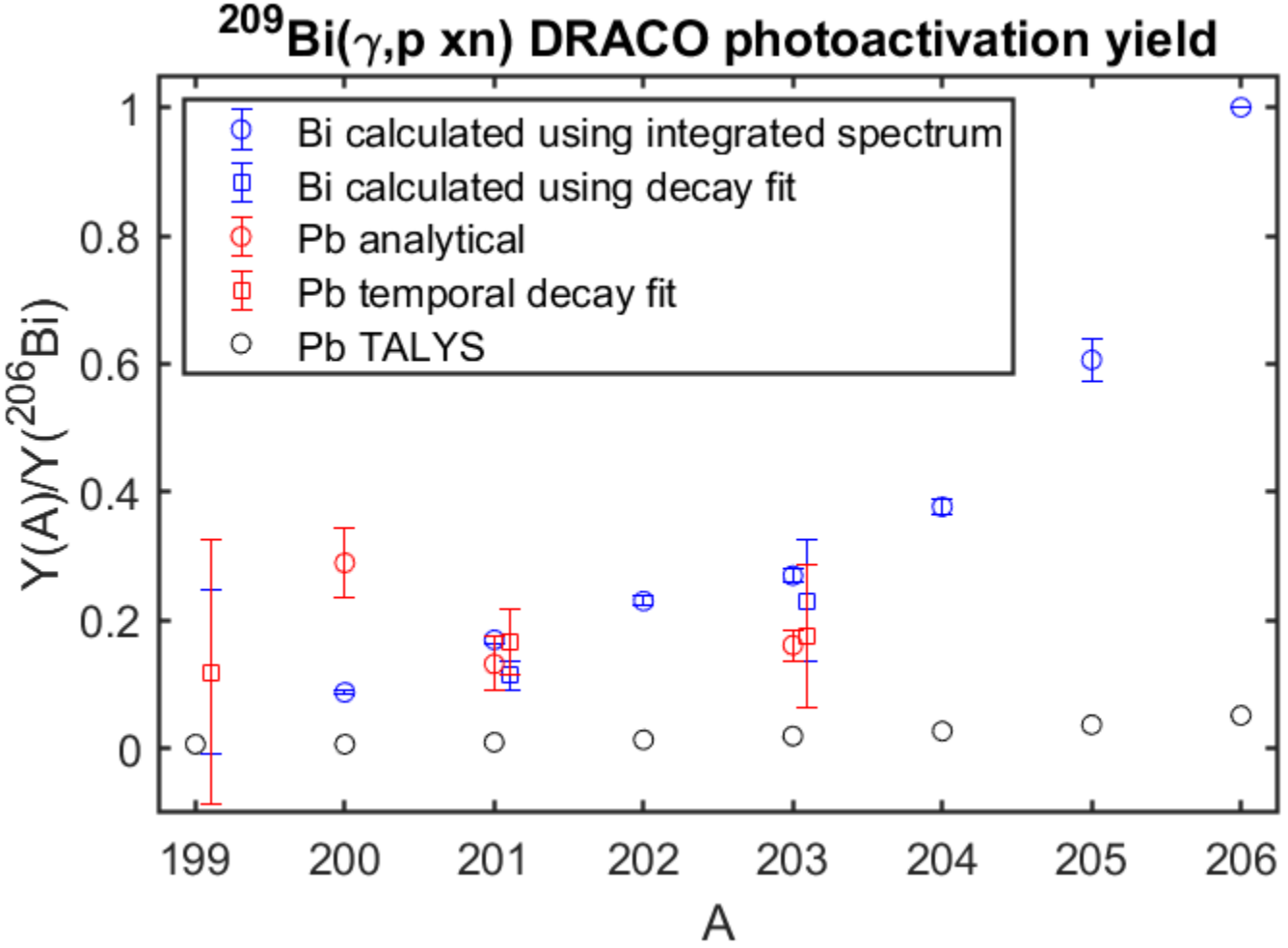

Yields of lighter elements

- The relative yields of Pb can be calculated using the same procedure as for Bi.
- TALYS simulations don't reproduce experiment.
- Same procedure can be used for some of the Thallium isotopes (γ,2pxn).

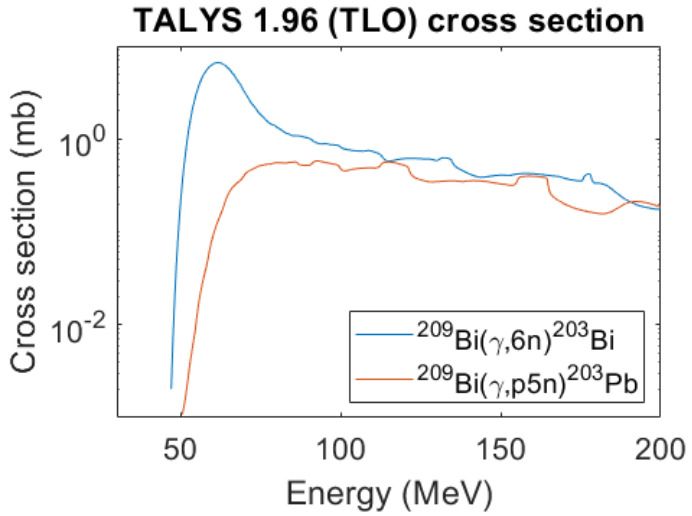

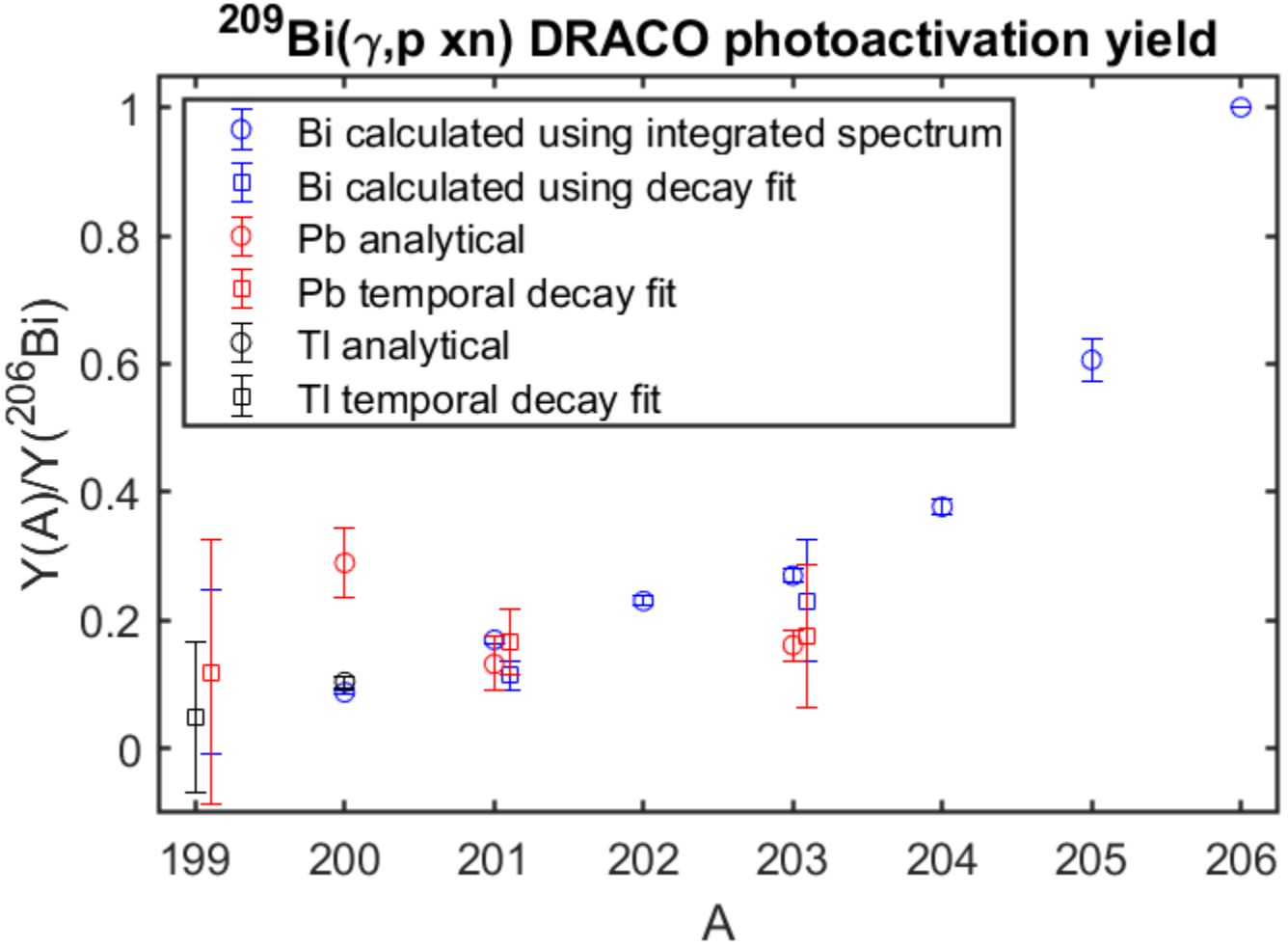

Conclusions

Conclusions

- Feasibility of laser-based facilities for nuclear research demonstrated.
- Successful photoactivation using high energy bremsstrahlung from the DRACO laser.
- Produced a short-lived activity of 10-100 Bq from 1-hour irradiation (300-400 shots).

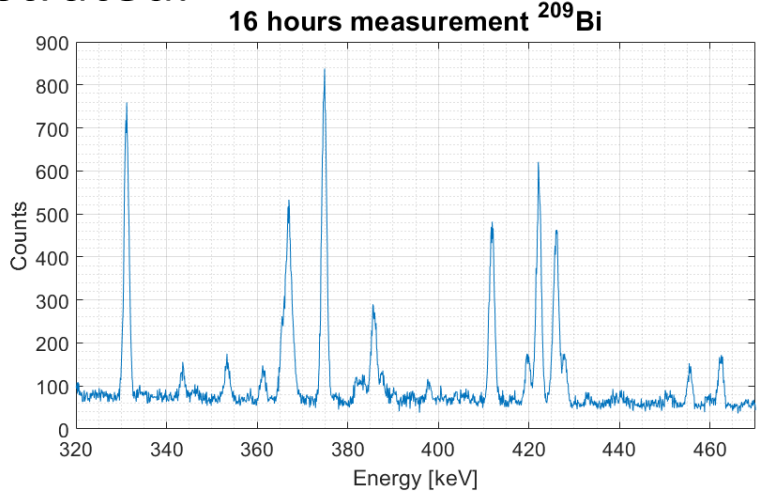

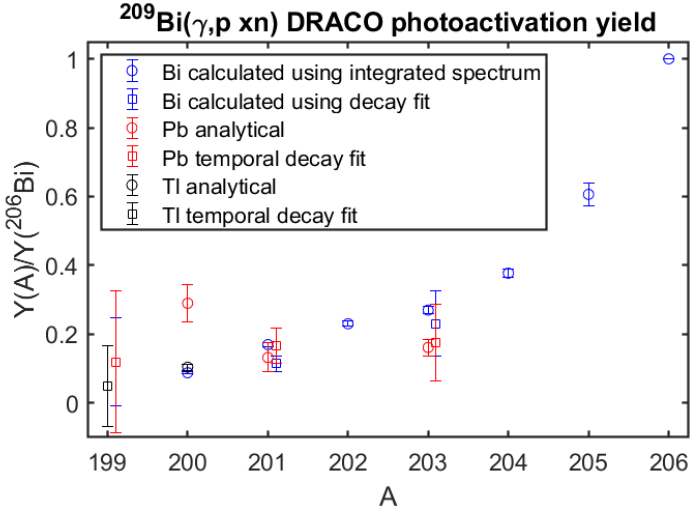

- Several isotopes of Bi were characterised.
- Additionally, lighter elements were directly generated, such as Pb or Tl, and their yield analysed.
- These experiments can be a useful tool for improving the simulation codes.

Adrián Bembibre Fernández: adrian.bembibre.fernandez@usc.es

Conclusions

- Feasibility of laser-based facilities for nuclear research demonstrated.
- Successful photoactivation using high energy bremsstrahlung from the DRACO laser.
- Produced a short-lived activity of 10-100 Bq from 1-hour irradiation (300-400 shots).

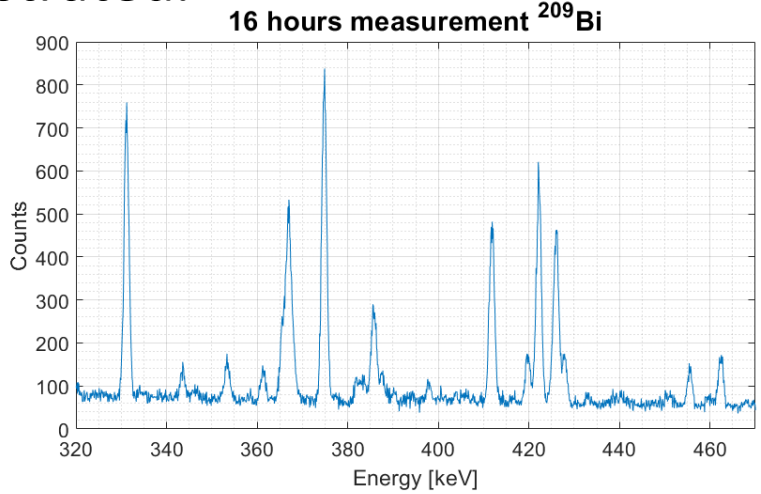

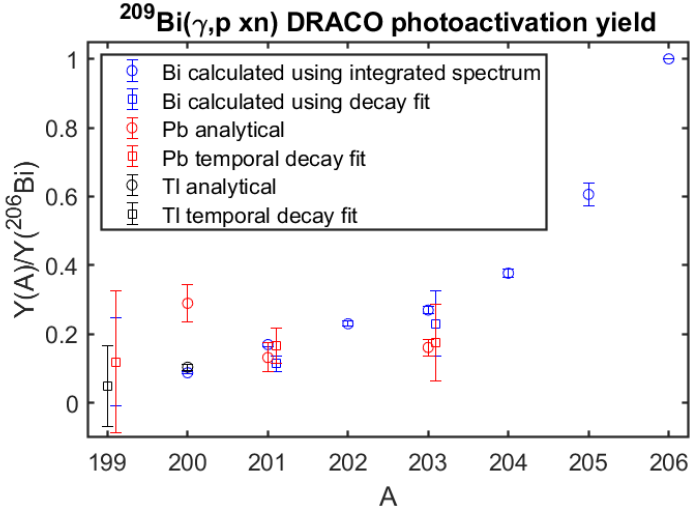

- Several isotopes of Bi were characterised.
- Additionally, lighter elements were directly generated, such as Pb or Tl, and their yield analysed.
- These experiments can be a useful tool for improving the simulation codes.

Thank you!

Adrián Bembibre Fernández: adrian.bembibre.fernandez@usc.es